Isospin symmetry breaking in mirror nuclei

S.M.Lenzi[1] and M.A.Bentley[2]

[1] Dipartimento di Fisica dell'Università and INFN, Sezione di Padova, I-35131 Padova, Italy `silvia.lenzi@pd.infn.it`

[2] Department of Physics, University of York, Heslington, York. YO10 5DD, U.K. `michael.bentley@york.ac.uk`

Abstract. Isospin symmetry is one of the fundamental symmetries we can identify in nuclei. This is related to the approximate charge symmetry and charge independence of the strong interaction. On this hypothesis, the level schemes of mirror nuclei (with exchanged number of protons and neutrons) should be identical. Of course some differences appear due to the fact that the Coulomb interaction breaks isospin symmetry. Energy differences between excited states in mirror nuclei can therefore be explained to a large extent in terms of the Coulomb effects. Recent investigations, however, suggest the need to introduce a non-Coulomb isospin symmetry breaking term to get a satisfactory quantitative description of the available data. In the last decade or so, the study of energy differences in isobaric nuclei as a function of angular momentum has been done systematically for nuclei in the $f_{\frac{7}{2}}$ shell. This has been possible due to important experimental developments in the identification of proton-rich nuclei produced with very low cross sections. Contemporaneously, state-of-the-art shell-model calculations have been produced for the description of these data. The synergy between theory and experiment for the study of energy differences of mirror and isobaric analogue nuclei has allowed the investigation of the evolution of the nuclear wave functions with increasing spin. The alignment process, related to changes of the spatial correlations of nucleons along a rotational band, together with changes of the nuclear radius or shape as a function of the angular momentum are examples of the type of phenomena that can be studied from the analysis of Coulomb energy differences. It is also possible to identify particular wave-function configurations of the states. In summary, the study of mirror energy differences has now become established as a very powerful tool to understand nuclear properties in nuclei. While most of the investigations so far have been concentrated mainly in nuclei of the $f_{\frac{7}{2}}$ shell, extensions to other shells are becoming available, which allows us to develop a more general view and description of the different properties that can be deduced from the data.

1 Introduction

The atomic nucleus is a complex quantum system formed by two different fermions, the proton and the neutron. Therefore, the theoretical description and interpretation of the properties of such a many-body system can be cumbersome. The identification of symmetries in the physics of the nucleus can help to understand the nuclear behavior, and constitutes a very powerful tool. Symmetries are intimately related to conservation laws and to conserved quantities which, in quantum mechanics, translate into good quantum numbers. Among the different symmetries that have been identified in nuclear physics, the *isospin* symmetry is

related to the identical behavior of protons and neutrons in the nuclear field. At the very beginning of nuclear physics only charged particles were known, but the nuclear mass could not be accounted for taking into account only these particles. In 1920, Rutherford suggested the existence of a neutral particle with a mass very similar to that of the proton and in 1932 Chadwick discovered the neutron. It was soon clear that the nuclear force acted similarly on protons and neutrons. This induced Heisenberg to propose treating them as the two quantum states of a particle called the *nucleon*. The quantum number associated to this symmetry was called "isospin" with the value $t = 1/2$, in analogy to the spin quantum number. Its projection on the z axis characterizes the two different nucleons: $t_z = -1/2$ for the proton and $t_z = 1/2$ for the neutron. In practice, the angular momentum algebra we know for treating the spin can be easily applied to isospin, but whereas the spin state of an elementary particle is determined by the projection of its spin in real space, the isospin state of the nucleon is determined by the projection in an abstract space: the isospin space. The isospin T of the nucleus is given by the vector sum of the single nucleon isospins. In a nucleus formed by N neutrons and Z protons the total projection $T_z = (N - Z)/2$ is well defined and therefore $|N - Z|/2 \leq T \leq (N + Z)/2$.

The strong interaction is, with good approximation, charge-symmetric and charge-independent. Charge-symmetric means that the interaction between two protons is identical to that between neutrons ($V_{pp} = V_{nn}$), while we say that it is charge-independent if $V_{pp} + V_{nn} = 2V_{pn}$. Of course, the Coulomb interaction breaks isospin symmetry as it acts only between protons. Putting the Coulomb interaction to one side, the concepts of charge symmetry and independence can result in identical behavior of two nuclei with the same total number of nucleons (*isobaric* nuclei), but with different numbers of neutrons and protons. Of course, the Pauli Principle puts obvious constraints on the available configurations and hence on the range of the symmetries observed. The isospin quantum number, T, directly couples together the two concepts of charge symmetry/independence and the Pauli principle. Isospin thus becomes a good quantum number to characterize analogue states in isobaric multiplets (Wigner, 1937). These states are termed *isobaric analogue states*, IAS, and the near-identicality of such states demonstrates the power of the isospin concept. In particular, nuclei with the same mass but with the numbers of protons and neutrons interchanged, *mirror nuclei*, would have identical structure, with all analogue states at the same excitation energy. Energy differences between IAS are due to isospin non-conserving forces, such as the Coulomb interaction.

For many decades the study of these energy differences was confined to low excitation energy and angular momentum [1]. Thanks to the advance in gamma-ray detection efficiency and resolving power achieved with large Ge multi-detector arrays, in combination with other ancillary devices it has been possible to extend these studies to high-spin yrast states. This allows to follow the IAS and their energy differences as a function of the angular momentum, and in particular, along the yrast line, that is the line that connects the lowest energy states at the highest angular momentum. The most studied isobaric multiplets are those of the $f_{\frac{7}{2}}$

shell, where collective structures have been observed up to the band-terminating states. The structure of these nuclei can be described with very good accuracy by the shell model. This has encouraged the extension of these calculations to the description of excitation energy differences between IAS to investigate the origin of isospin-symmetry-breaking (ISB) effects. It turns out that such energy differences – usually called Coulomb energy differences (CED) – yield detailed information on changes in *nuclear* structure with increasing energy and angular momentum. More recently, experimental and theoretical efforts have allowed to extend these studies to nuclei in the sd and upper fp shells. In these lectures the CED in the region of nuclei between $A \sim 40$ and $A \sim 60$ will be discussed in detail.

We will start with the description of some properties of the isospin symmetry and the application of the isospin concept to energy differences between analogue states in isobaric multiplets. Technical developments in both experimental techniques and the nuclear shell model that have enabled the rapid progress in this field will then be discussed. Finally, some examples of the experimentally measured energy differences that show the role of the different terms that contribute to the energy differences will be presented.

2   The isospin symmetry in isobaric multiplets

2.1   Basic concepts

The general concept of the charge invariance of the nuclear force can be subdivided into two properties: charge symmetry and charge independence. As stated above, charge symmetry requires that the nuclear proton-proton interaction (V_{pp}) is equal to that between neutrons, V_{nn}. Recently, accurate data of nucleon-nucleon scattering experiments have shown evidence for a slight charge asymmetry in the measured scattering lengths of -18.9 ± 0.4 fm (nn) and -17.3 ± 0.4 fm (pp) [2]. Of course, these data refer to free-nucleon interactions, and not to the effective nucleon-nucleon interaction in the nuclear medium. The origin of the observed charge-symmetry breaking (CSB) is not yet fully settled, and models based on the effects of nucleon mass splitting and meson mixing have been applied to this problem ([2,3], and references therein). The more stringent condition of charge-independence also requires that $(V_{pp} + V_{nn})/2 = V_{np}$, which is also known to be broken slightly [4]. Nevertheless, the concepts of charge symmetry and charge independence will be expected to result in clear symmetries in the nuclear behavior.

Isospin selection rules put some constrains to the electromagnetic transitions and the weak interaction. Certain decays are forbidden if isospin is a good quantum number for hadronic forces. In particular, electromagnetic $E\lambda$ and $M\lambda$ transitions can only connect states with $\Delta T = 0, \pm 1$. Electric $E1$ transitions between $\Delta T = 0$ states are forbidden in $N = Z$ nuclei, and have equal strengths in mirror nuclei. Quadrupole $E2$ transitions have a linear dependence on T_z in an isobaric multiplet. Moreover, magnetic $M\lambda$ transitions between states of the

same T in an $N = Z$ nucleus are hindered. For the beta-decay, Fermi transitions are allowed only along isobaric multiplets.

The value of T is not an observable quantity, though for nuclei near $N = Z$ (where the concept of isospin is most relevant) it can usually be "assigned" using logical arguments. This can be done easily if it is remembered that states of a given T can only occur in a set of nuclei with $T_z = T, T-1, ..., -T$ (since $|T_z| > T$ is forbidden). We start our consideration of isospin with the simplest systems, formed by two nucleons: nn, pp and np. Here, T_z is $0, \pm 1$ and so the value of T is restricted to 0 and 1. Charge-independence dictates that any state that can be constructed in the pp (or nn) system must also exist in the np system. However, the inverse statement *cannot* be made. That is, there are some states in the np system that are forbidden by the Pauli principle in the pp (or nn) system composed by identical particles. The ground state of the deuteron (np) with $J^\pi = 1^+$ is such a state and, therefore, *must* have $T = 0$ as the isospin projection is limited only to $T_z = 0$. Similarly, any state in the nn system (and its equivalent state in pp) must have $T = 1$ as the projection is $T_z = 1$ (-1 for pp). However, as a $T = 1$ state can have a $T_z = 0$ projection, this state *must* also exist in the np system. Thus, there are three identically-constructed $T = 1$ states which can be found in the nn, np and pp systems (i.e. with $T_z = 1, 0, -1$ respectively). These states form an *isospin triplet*, and the lowest $J^\pi = 0^+$ states in these three two-nucleon systems form such a triplet. In fact, as we know, all three of these states are unbound. This classification argument can easily be extended to states in many-particle systems, where it is also useful to remember that, in general, the lowest energy states (e.g. the ground state) of a nucleus will have the lowest available value of isospin (i.e. $T = |T_z|$) (Exceptions to this "rule" are, for example, $N = Z$ odd-odd nuclei in the $f_{\frac{7}{2}}$ shell and ^{34}Cl, where $T_z = 0$ and the ground state has $T = 1$.) Thus, for example, one finds four nuclei with $T_z = \pm\frac{1}{2}, \frac{3}{2}$ all four of which contain an identically-constructed $T = \frac{3}{2}$ state – an isospin quadruplet. The two "outer" nuclei with $T_z = \pm\frac{3}{2}$ have $T = \frac{3}{2}$ ground states (which are mirror states - see below), and for the other two nuclei with $T_z = \pm\frac{1}{2}$ the $T = \frac{3}{2}$ analogue states are excited states, as the ground states of these two nuclei will be expected to have $T = \frac{1}{2}$.

The simplest example of an isobaric multiplet is a pair of mirror nuclei. In a mirror pair, the total number of pp interactions in one member of the pair is the same as the number of nn interactions in the other. Hence only the charge-*symmetry* of the nucleon-nucleon interaction is required to provide isospin symmetry in a mirror pair. This is generally not the case for any set of IAS, where the isospin symmetry across a multiplet relies on both charge symmetry *and* charge independence. Let's look at the isobaric triplet of mass $A = 22$ formed by the odd-odd $N = Z$ nucleus ^{22}Na and the two mirrors ^{22}Mg ($Z = 12$) and ^{22}Ne ($Z = 10$) (Fig. 1). As in the case of the deuteron, the ground state of ^{22}Na is a $T = 0$ state, but the spin and parity are $J^\pi = 3^+$, as the odd proton and neutron are filling the $d_{\frac{5}{2}}$ orbital and the nucleus is deformed. The first $T = 1, J^\pi = 0$ state lies at 693 keV excitation energy and is the isobaric analogue state of the ground states of ^{22}Mg and ^{22}Ne. Due to the Pauli Principle,

the N=Z nucleus has more excited states than the other members of the triplet. The small differences between the excited states are a consequence of the effect of the isospin breaking terms of the interaction such as the Coulomb force. Once this effects are taken into account, the size of remaining differences constitutes a test of the charge independence of the nuclear interaction.
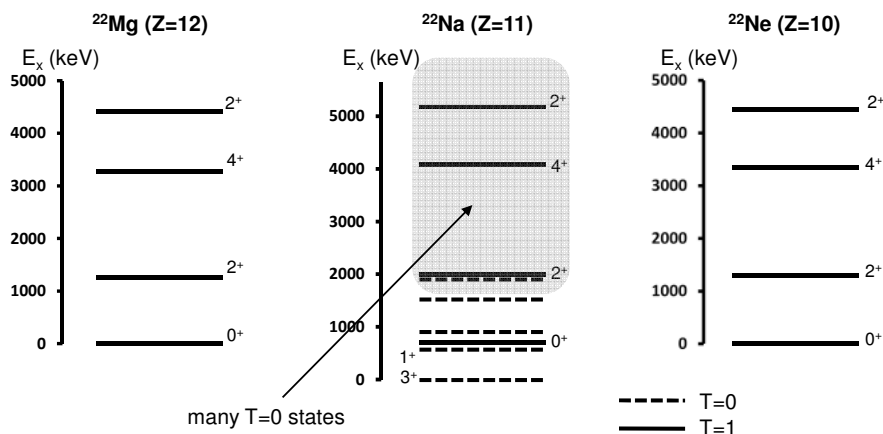

Fig. 1. The isobaric triplet $A = 22$

Another interesting case of isospin triplet is that formed by the $N = Z$ ^{20}Ne, and the odd-odd ^{20}Na (Z=11) and ^{20}F (Z=9). Also here, the g.s. of ^{20}Ne is a $T = 0$ state, but the first $T = 1$ state, analogue to the ground state of the other two members of the triplet lies at 10723 keV. This is much higher than in the previous example just due to the fact that in odd-odd N=Z nuclei $T = 0$ and $T = 1$ states lie nearer in energy (in heavier nuclei the lowest state is in general a $T = 1$ state). As a last example we take the isospin quadruplet of mass $A = 21$. This quadruplet is formed by ^{21}F, ^{21}Ne, ^{21}Na and ^{21}Mg. The nuclei (mirror) ^{21}Ne and ^{21}Na have $T_z = \pm 1/2$, while ^{21}F and ^{21}Mg have $T_z = \pm 3/2$. Therefore, there will be $T = 1/2$ states in the first pair and $T = 3/2$ states in all members of the quartet. We expect, however, that the $T = 3/2$ states will be higher in energy in the $T_z = \pm 1/2$ pair. The level schemes of the isospin quarter is reported in Fig. 2. In this figure, as in the previous one, the ground states and/or the lowest states for a certain isospin multiplet are put at the same level. This allows a clear comparison of the level schemes and to appreciate the small differences in the excitation energy of analogue states. The study of these differences, called Coulomb energy differences (CED), mainly due to the effect of the electromagnetic interaction, is the main subject of these lectures. These energy differences are of the order of tens of keV. In the following paragraph, on the other side, we discuss the differences in the binding energy of analogue states

in a multiplet, that is, we do not refer to the excitation energy with respect to
the ground state but consider the absolute binding energy of the states. These
differences are called Coulomb displacement energies (CDE) and amount to the
order of tens of MeV. As we will see, there is a very simple formula that largely
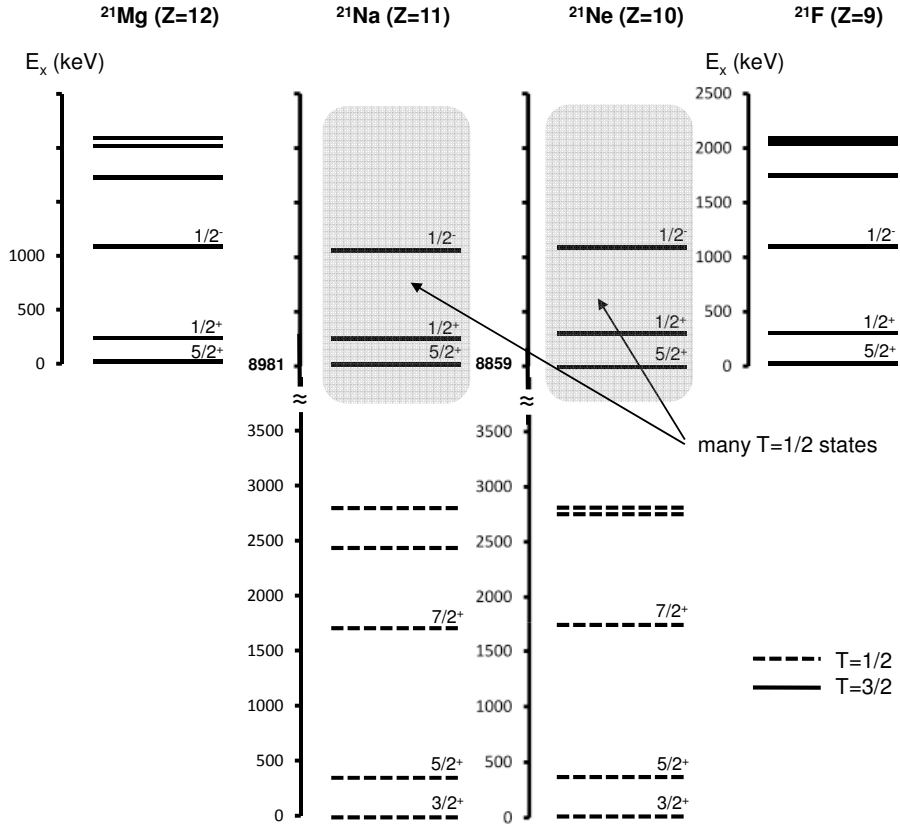accounts for these differences.

Fig. 2. The isobaric quadruplet $A = 21$

2.2   Coulomb Displacement Energies and the Isobaric Multiplet Mass Equation

The difference in binding energy of two nuclei (CDE), members of an isobaric
multiplet, can be obtained from the mass difference (there is only a change in the
sign). Based on the concept of isospin symmetry, in nuclear physics, E.P. Wigner
introduced in 1957 [5] the so-called isobaric multiplet mass equation (IMME).

This is a fundamental prediction that describes the dependence of the mass (or binding energy) of a set of IAS with Z (or T_z). The largest effect on the CDE is always due to the Coulomb interaction, which lowers the total binding energy of a state in one member of the multiplet relative to the IAS in the neighbouring lower-Z isobar.

A full description of the IMME can be found in several papers and reviews (e.g. [1,6–8]). We present an outline derivation of the IMME here, as it serves as an example of the power of the isospin formalism. We start with the eigenstates $|\alpha T T_z\rangle$ of the charge-independent Hamiltonian H_{CI}, where α contains all the additional quantum numbers that define the state. Since H_{CI}, by definition, conserves T, the eigenvalues are independent of T_z - i.e. the isobaric analogue states are completely degenerate. A charge-violating interaction will lift this degeneracy and can be treated as a perturbation if the total energy splitting induced is small compared with the binding due to the nuclear force – as is the case with the Coulomb interaction. The total binding energy can be determined by:

$$BE(\alpha T T_z) = \langle \alpha T T_z | H_{CI} + H'_{CV} | \alpha T T_z \rangle \tag{1}$$

where H'_{CV}, represents the charge-violating interaction(s). If two-body forces alone are responsible for the nature of H'_{CV}, then it can be written as,

$$H'_{CV} = \sum_{k=0}^{2} H_{CV}^{(k)} \tag{2}$$

where $k = 0, 1, 2$ correspond to the isoscalar, isovector and isotensor components of this interaction respectively. The total energy splitting of the isobaric multiplet is given by

$$\Delta BE(\alpha T T_z) = \langle \alpha T T_z | \sum_{k=0}^{2} H_{CV}^{(k)} | \alpha T T_z \rangle. \tag{3}$$

The application of the Wigner-Eckart theorem can then extract explicitly the T_z-dependence of the energy splitting of the multiplet:

$$\Delta BE(\alpha T T_z) = \sum_{k=0}^{2} (-)^{T-T_z} \begin{pmatrix} T & k & T \\ -T_z & 0 & T_z \end{pmatrix} \langle \alpha T \| H_{CV}^{(k)} \| \alpha T \rangle \tag{4}$$

where the double-bars in the final term denote matrix elements reduced in isospin. The above Wigner $3 - j$ symbols for the three values of k have well known analytic forms, and we obtain

$$\begin{aligned}
\Delta BE(\alpha T T_z) &= \frac{1}{\sqrt{2T+1}} [M^{(0)} \\
&\quad + \frac{T_z}{\sqrt{T(T+1)}} M^{(1)} \\
&\quad + \frac{3T_z^2 - T(T+1)}{\sqrt{T(T+1)(2T+3)(2T-1)}} M^{(2)}] \\
&= a + bT_z + cT_z^2 \tag{5}
\end{aligned}$$

where $M^{(k)}$ are the three sets of reduced matrix elements $\langle \alpha T \| H_{CV}^{(k)} \| \alpha T \rangle$, the values of which are independent of T_z but otherwise dependent on T and α.

With this re-ordering of the terms, the IMME acquires a quadratic form. The conclusion then is that the binding energy splitting (and hence mass) of an isobaric multiplet is quadratic in T_z where the coefficients a, b and c depend only on T and sets of reduced matrix elements. In addition, the derivation of Eq. (5) shows that the coefficients are directly related to the three tensor components of the interaction. The a coefficient depends mostly on the isoscalar component, with a small contribution from the isotensor one. The b and c coefficients are related only to the isovector and isostensor components, respectively. Put another way, the values of b and c (which can be determined experimentally) can potentially yield separate information on the charge-symmetry and charge-independence, respectively, of the attractive nucleon-nucleon interaction.

The IMME is valid in the presence of *any* charge-violating (i.e. isospin non-conserving) interaction or set of interactions, provided they are of two-body character. Of course, the Coulomb interaction is expected to be the dominant contributor. However, the quadratic nature of the IMME would be valid even in the presence of charge-asymmetric and charge-dependent components of the attractive nucleon-nucleon potential. Only the values of the coefficients would be affected by the presence of such effects. Deviations from IMME would be expected, of course, if higher-order perturbations and/or the inclusion of three-body terms are important. In addition, as pointed out by Auerbach [9], a significant component of isospin mixing could also result in deviations from the IMME quadratic behaviour.

As the IMME is such a basic prediction leading from the isospin concept, testing the validity of the equation is clearly of fundamental importance. The most effective way is examine isobaric multiplets with at least four members (i.e. $T \geq \frac{3}{2}$), and fitting a cubic expression by inclusion of a $d\, T_z^3$ term. Of course, the value of the d coefficient should be consistent with zero if the quadratic nature of the IMME is valid. New experimental data are available that have now allowed the validity of the IMME to be tested this way – see Britz, Pape and Anthony [10] for a comprehensive compilation. Fig. 3 contains data taken from Ref. [10] for all the known $T = \frac{3}{2}$ isobaric quadruplets. Firstly, Fig. 3 clearly shows that the d coefficients, extracted from the data following the cubic fit described above, have values consistent with zero over all the measured masses so far. Thus, the agreement with the prediction of the quadratic nature of the IMME is quite remarkable. Only one exception appears, once the magnitude of the error bars is taken into account, that of the $T = \frac{3}{2}, J^\pi = \frac{3}{2}^-$ isobaric quadruplet for A = 9. In recent experiments of mass measurements in the A=32 quartet, the data do not agree with the quadratic form of the IMME and a cubic term has been introduced to fit the data [11]. This cubic term has been suggested to be due to isospin mixing of the states, second-order Coulomb effects and charge-dependence of the nuclear interaction [11].

The coefficients of the IMME can be determined experimentally but this does not yield any direct information on the nature of the two-body interaction. Put
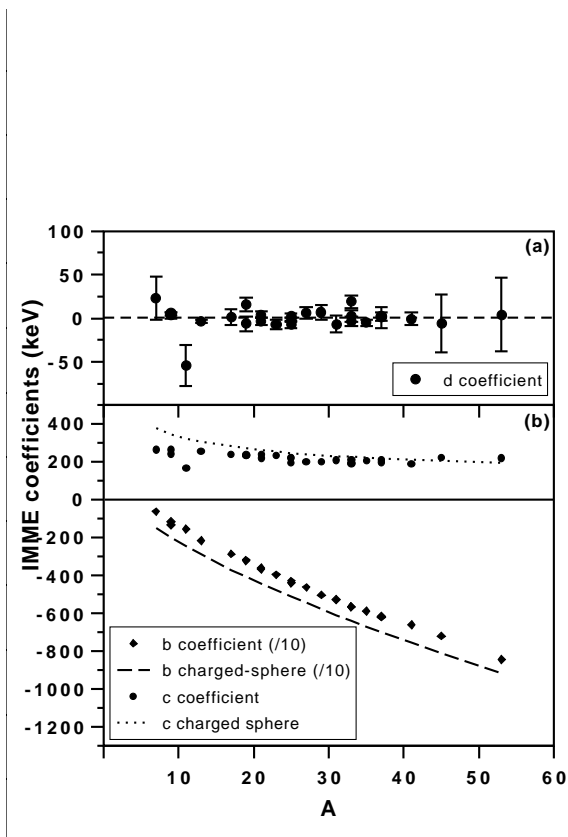
Fig. 3. Coefficients of the IMME of the form $BE(T, T_z) = a + bT_z^2 + cT_z^2 + dT_z^3$ obtained from fits to experimental data for $T = \frac{3}{2}$ quadruplets (data taken from [10]). The experimentally determined b, c and d coefficients along the predictions of the simple charged sphere model - see text and Eq. (7) - where r_0 is taken to be 1.2 fm.

another way, a detailed understanding of the charge-violating components of the interaction is required to reproduce theoretically the values of the coefficients of the IMME. Here we make a rough estimate of the coefficients taking into account only the Coulomb interaction as the isospin breaking force.

Assuming that the nucleus can be treated as a uniformly charged sphere, we derive a simplistic estimate of the coefficients of the IMME as a function of mass. The Coulomb energy of such a uniformly charged sphere is given by

$$E_C = \frac{3e^2 Z(Z-1)}{5R_C} = \frac{3e^2}{5r_0 A^{\frac{1}{3}}} \left[\frac{A}{4}(A-2) + (1-A)T_z + T_z^2 \right]. \qquad (6)$$

Hence we arrive at the expressions

$$a = \frac{3e^2 A(A-2)}{20r_0 A^{\frac{1}{3}}}, \; b = -\frac{3e^2(A-1)}{5r_0 A^{\frac{1}{3}}}, \; c = \frac{3e^2}{5r_0 A^{\frac{1}{3}}}. \qquad (7)$$

The predictions of this crude estimate are shown in Fig. 3 along with the b and c coefficients extracted from the $T = \frac{3}{2}$ isobaric quadruplets [10]. We note that the proton-neutron atomic mass difference Δ_{nH} also contributes to the b coefficient, and the prediction has been modified to account for this. The overall magnitude and trends of the charged-sphere prediction are clearly fairly good, although there is a ≈ 1MeV over-estimate of the magnitude of the b term. As has been known for a long time (e.g. Bethe and Bacher 1936 [12]) such classical estimates of the Coulomb energy stored in a nucleus need to be modified to account for the effect of antisymmetrisation. Effectively, the average result of the Pauli principle is to keep the protons further apart than would be allowed classically, and this accounts for at least some of the discrepancy in the b coefficient in Fig. 3.

The total binding energy difference (Coulomb Displacement Energy, CDE) between a particular state and its analogue state in another member of the isospin multiplet of isospin T, transformed through exchange of k protons for neutrons is given by

$$CDE(T, T_z) = M_{T,T_z} - M_{T,T_z+k} + k\Delta_{nH} \qquad (8)$$

where M is the atomic mass (that includes the excitation energy of the state on interest if this is not the ground state), Δ_{nH} is the neutron-Hydrogen atomic mass difference and T_z is the isospin projection for the larger-Z isobar.
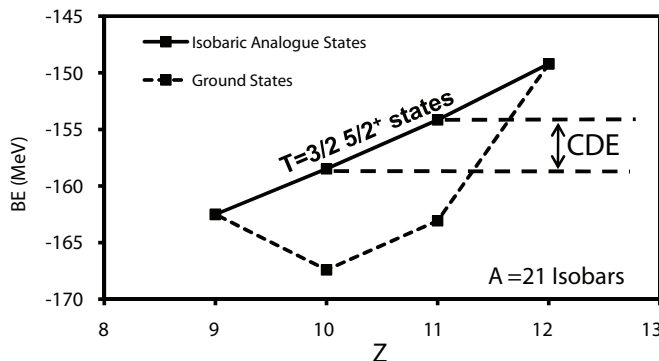
Fig. 4. The experimental binding energies of the $A = 21, T_z = \pm\frac{1}{2}, \pm\frac{3}{2}$ nuclei – both for the ground states and for the $T = \frac{3}{2}$ isobaric analogue states. The Coulomb Displacement Energy (CDE) between adjacent members of the $T = \frac{3}{2}$ quadruplet is indicated.

An example is shown in Fig. 4 for the $A = 21$ isobars with $T_z = \pm\frac{1}{2}, \frac{3}{2}$, where the ground-state binding energies form the usual Weizsäcker parabola. The $T = \frac{3}{2}$ isospin quadruplet shown includes the ground states of the two $T_z = \pm\frac{3}{2}$ nuclei, and the corresponding excited (isobaric analogue) states of the two nuclei in between. We have seen above, in the discussion of the IMME, that the binding energies of the IAS are *also* parabolic in Z – the dashed line in Fig. 4. The CDE indicated is the total binding energy difference between the two neighbouring members of the multiplet. Here, as is conventional, we associate the CDE specifically with the lowest-energy set of IAS in a multiplet, whilst keeping in mind that bound excited-state sets of IAS will also exist in all probability in the multiplet.

In a refined calculation, the CDE is the most basic quantity one would want to reproduce theoretically. The CDE is, of course, directly related to the IMME coefficients: for any two IAS in a multiplet we have

$$CDE(T, T_z) = -p(b + c[2T_z + p] - \Delta_{nH})$$ (9)

where again we have exchanged p protons for neutrons and T_z is the isospin projection for the larger-Z isobar. The CDE has been the subject of much theoretical work – most notably the reviews of Nolen and Schiffer [13], Shlomo [14] and Auerbach [9]. In these reviews, CDE have been calculated for wide ranges of IAS for which experimental data exist for comparison. In the original work of Nolen and Schiffer [13], a charge-symmetric and charge-independent interaction was assumed – and thus it is assumed initially that b and c originate *entirely* from the Coulomb interaction. The difference in Coulomb energy between adjacent members of the multiplets was computed using independent particle models. Here the dominant Coulomb shift was determined by computing the density distribution of the neutron excess in one member of the multiplet, and calculating the Coulomb shift when one of the neutrons is transformed into a proton. To this are added two further contributions - an exchange term (the result of the Pauli effect described above) and an *electromagnetic* spin-orbit term. The latter term turns out to be very significant in the interpretation of excited states energy differences, and we will discuss this later. These three terms combined do not account fully for the experimental CDE, and so a number of corrections were computed. The largest corrections included the Coulomb distortion of analogue wavefunctions, isospin impurities in the core and intrashell interactions. When all the corrections were taken into account, there remained a consistent under-estimate of the CDE by around 7% on average - amounting to several hundred keV. This is the so-called "Nolen-Schiffer" anomaly. Much theoretical work on this anomaly has followed – especially in the comprehensive reviews of Shlomo [14] and Auerbach [9]. Here the calculations were revisited and refined, and further corrections were introduced - including effects associated with configuration mixing and polarisation of the core due to particle-vibration coupling.

Further studies have identified a number of phenomena that could account for the discrepancy. For example, it has been suggested [15,16] that this anomaly could be principally associated with a charge-asymmetric component of the

nucleon-nucleon interaction although Shlomo earlier showed [14] that this can only account for about half of the discrepancy in heavy nuclei, and that the effect of differences in neutron a proton radii could contribute significantly to the anomaly. Duflo and Zuker [17], studying the neutron skin, also show that a proper quantum treatment of the Coulomb and charge-symmetry breaking interactions gives a very good description of the CDE, reducing the anomaly significantly. Whatever the source of the Nolen-Schiffer anomaly, it seemed from these studies that a detailed structural understanding of Coulomb effects at the level of less than, say, 100 keV was likely to be very difficult.

2.3   Energy differences between excited IAS.

We come now to the main subject of these lectures: The differences in *excitation* energy between excited IAS, generically termed Coulomb Energy Differences or CED. In determining CED between excited states, we effectively "normalise" the absolute binding energies of the ground states, thus the CED only reflect the *change in CDE* in relation to the ground state. The bulk of the CDE (e.g. the difference in bulk Coulomb energy) will simply cancel in this process. The CED between IAS in two members of a multiplet obtained through exchanging k protons for neutrons is given generically by

$$CED_{J,T} = E^*_{J,T,T_z} - E^*_{J,T,T_z+k}.$$ (10)

It is interesting to examine how the Coulomb energy (and other charge-dependent phenomena) vary as a function of excitation energy and angular momentum (spin) for a set of IAS. In particular, the IAS are expected to show slight differences with increasing spin associated with the influence on the Coulomb energy of the changing of the wave functions of the excited states. These measured CED are typically 100 keV or less and, due to these small values, are remarkably sensitive to quite subtle nuclear structure phenomena which, with the aid of shell-model calculations, can be interpreted quantitatively at the level of 10 keV. This is especially true when we restrict the study to excited structures in nuclei whose wave functions have major contributions from a single-j shell - such as in the $f_{\frac{7}{2}}$-shell. In these cases, the CED can be reliably interpreted in terms of structural phenomena such as changes in the spatial correlations of pairs of valence protons and/or changes in radius/deformation as a function of spin. When the excitations involve significant changes in the single-particle contributions to the configurations, then larger CED (few hundred keV) can be observed. This, in turn, yields valuable information on the single-particle structure of the states and the nature of the excitations involved.

In the last decade, the study of CED between IAS has been pursued in considerable detail, yielding some remarkable results. This has been possible due to important developments in both theoretical and experimental techniques. It has been possible to examine CED between many $T = \frac{1}{2}$ doublets and $T = 1$ triplets up to the highest accessible excitation energy and angular momentum and more recently, these studies have been extended to $T = 3/2$ and $T = 2$ IAS,

using radioactive beams. The most extensively studied cases are the $T_z = \pm\frac{1}{2}$ isobaric doublets (mirror pairs), where the CED can be followed up to very high spin states. For a pair of mirror nuclei, the CED are specifically referred to as mirror energy differences (MED), defined, for any pair of mirror nuclei, as the difference in excitation energy as a function of spin:

$$MED_{J,T} = E^*_{J,T,T_z=-T} - E^*_{J,T,T_z=T} = -k\Delta b_J \qquad (11)$$

where we have assumed that the lowest isospin states are being studied – i.e. $T = |T_z|$. Here, again, k protons have been exchanged for neutrons, and in this specific case $k = 2T = 2|T_z|$. Here, we have used Eq. (5) to link the MED to the coefficients of the IMME, and we define Δb_J as the change in the b coefficient as a function of spin in relation to the ground state. We see that the MED give us *isovector* energy differences, the interpretation of which relies entirely on the concept of charge-*symmetry*.

To test the charge-*independence* of the interaction we consider an isobaric $T = 1$ triplet (i.e. $T = 1, T_z = 0, \pm 1$). The triplet energy differences (TED) are defined as

$$TED_J = E^*_{J,T_z=-1} + E^*_{J,T_z=+1} - 2E^*_{J,T_z=0} = 2\Delta c_J, \qquad (12)$$

where we see that the TED depend only on the variation of the c coefficient with spin, hence these *isotensor* energy differences yield information on the Coulomb energy if charge *independence* of the nuclear interaction is assumed (cf. charge-*symmetry* for MED). Conversely, deviations of the calculations from the experimental data will give evidence of violations of the charge symmetry and/or charge independence of the nuclear interaction. This turns out to be, however, quite difficult. For example, one essential ingredient in modelling Coulomb phenomena is the set of matrix elements that describe the Coulomb energy of a pair of protons as a function of their angular momentum – Coulomb Matrix Elements, CME. These either have to be modelled or extracted from the data – neither of which is particularly reliable. Nevertheless, a consistent picture of spin-dependent Coulomb phenomena (and other isospin non-conserving effects) is now emerging, which is discussed in the following sections.

3   Experimental tools

In terms of the experimental tools used to study such isobaric analogue states, we find that it is no coincidence that the rapid progress in spectroscopy of excited states in proton-rich nuclei happened at the same time as the development of large Compton-suppressed gamma-ray spectrometers. A good review can be found in Lee *et al.* [18] for the arrays used with stable beams and fusion-evaporation reactions - such as the Gammasphere array [19], (based in the US at either the Lawrence Berkeley National Laboratory or the Argonne National Laboratory), the European spectrometer Euroball [20,21] (based at either IReS Strasbourg or Legnaro National Laboratory) and the GASP array [22] based at

Legnaro National Laboratory. With radioactive (fragmentation or ISOL) beams arrays such as Exogam [23], RISING [24] or SeGA [25] have been more recently used. These are all arrays of hyper-pure germanium detectors (HpGe) – either single-crystal or composite detectors and are based on the principle of maximising the total gamma-ray detection efficiency whilst maintaining a sufficient granularity to enable multiple gamma-ray coincidences to be recorded and to reduce the probability of more than one gamma ray hitting any crystal.

For studying proton-rich nuclei at the extremes of stability the resolving power of these arrays is not usually sufficient to extract the weak gamma-ray signals from the data. Thus highly selective ancillary detectors for identifying the final nucleus are normally employed - and this information is used to "tag" the observed gamma decays. This is essential for proton-rich nuclei, where cross sections in fusion-evaporation reactions are no higher than the millibarn level (i.e. roughly 1 reaction in 10^3 leading to the nucleus of interest) down towards the few *microbarn* level. Moreover, in general, no gamma-ray transitions will have been identified previously in that nucleus. Thus, we require high gamma-ray efficiency and clean nucleus identification to measure weak gamma-ray transitions *and* assign them to a particular nucleus. Below we discuss two different examples, both using large gamma-ray arrays but each using a different reaction-channel selection method. The first uses stable beams, and the second relativistic fragmentation beams.

The first method discussed here is the selection of weak reaction residues from fusion evaporation reactions using stable beams through A and Z determination of the recoiling nucleus. This requires a $0°$ mass separator downstream of the target, coupled to a device for determining Z. The example shown here is the identification of excited states in $T_z = -1$ ^{44}V [26], for which the Argonne Fragment Mass Analyser (FMA) was used in conjunction with the Gammasphere array. The FMA uses a combination of electric and magnetic dipoles to give velocity selection to remove the beam particles and provide dispersion in A/Q (Q being the atomic charge state). A/Q is therefore determined on an event-by-event basis from the horizontal position at the focal plane - thus providing an initial mass measurement. For low cross-section studies of proton-rich nuclei, determination of A is not sufficient and nuclear charge is required. For the ^{44}V case, and other studies such as the A=48 $T = 1$ mirrors [27] this was achieved using a split-anode ionisation chamber after the focal plane. The chamber is filled with isobutane gas, enabling energy loss in the first part of the chamber (ΔE), in addition to the total energy (E) to be recorded. Two-dimensional gates on such a plot provide a clean selection on Z as long as the recoils have sufficient energy.

For the ^{44}V experiment, the reaction used was ^{36}Ar(^{10}B,$2n$)^{44}V at a beam energy of 95 MeV and was ideal for this purpose as the recoiling ^{44}Mn nuclei were highly energetic due to the inverse nature of the reaction. Thus, the different Z values in the Ion Chamber spectra were distinct and clean gates could be placed without the need for tricky background subtractions. However, even in this case, the A and Z selection methods described above were insufficient due
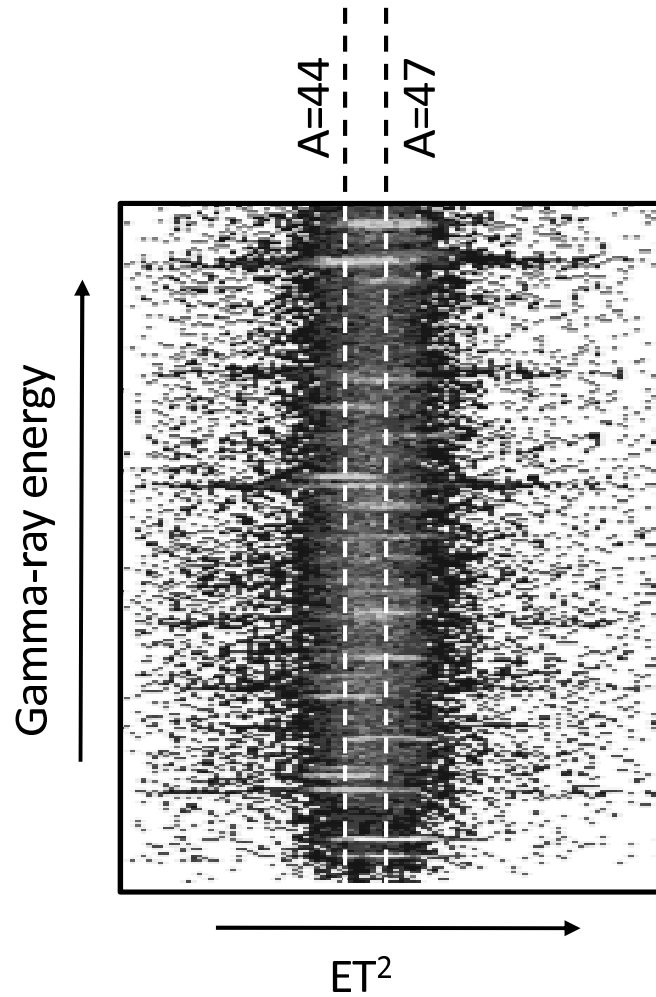
Fig. 5. A plot of gamma-ray energy measured using Gammasphere versus ET^2 measured for the nuclei recoiling through the FMA for the ^{44}V experiment – see text. The plot was created selecting $A/Q \approx 3$ which allows $A = 44$ and $A = 47$ recoils through in charge states 15 and 16 respectively. The plot also is gated on $Z = 23$ from the ionisation chamber. The lines indicate the expected positions for the A=44 desired recoils and the A=47 contaminants,

to the very low (few hundred μb) cross-section. In the experiment, reactions with the very low levels of oxygen contamination on the target were many times stronger than the reactions of interest, and the main contaminant (^{47}V from the ^{36}Ar$(^{16}$O$,\alpha p)^{47}$V reaction) had a value of A/Q similar to that of the charge-state

of ^{44}V selected. This isobaric contamination is well known in separator physics and is known as a charge-state ambiguity. Such ambiguities can be removed by using the recorded total energy E and time-of-flight T of the recoils. Classically, mass is proportional to ET^2, and the recorded ET^2 information has sufficient resolution to distinguish three mass units difference. This can be seen from Fig. 5 where an ET^2 versus gamma-ray energy plot is provided. This has been created requiring $A/Q \approx 3$ and $Z = 23$. The two lines indicate the expected positions of the ^{44}V required recoils and the ^{47}V contaminants. When an additional ET^2 gate is applied, following suitable background subtraction, the spectrum of the lower part of Fig. 6 is finally obtained. The gamma rays can now be entirely associated with ^{44}V – the excited states for which are largely unknown. The ^{44}Sc spectrum, produced the same way, is shown in the upper spectrum of Fig. 6. The comparison shows the expected mirror symmetry, and comparison of the upper and lower spectra enables assignments of energies and angular momenta on mirror symmetry arguments. It is interesting to note the factor of 1000 in the cross sections between the two nuclei in this reaction.
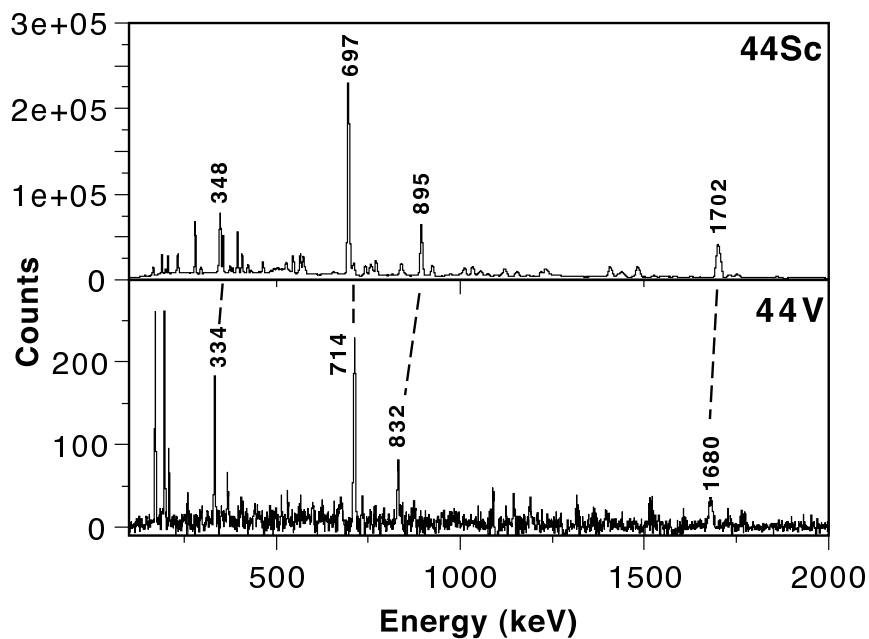
Fig. 6. The spectra for the ^{44}V experiment using Gammasphere and the FMA. These have been generated following selection for $A/Q \approx 3$, Z=23 (lower) and Z=21 (upper) and an appropriate gate on ET^2 to remove charge-state ambiguities. The four transitions marked are analogue transitions, with the assignments in ^{44}V made through mirror symmetry arguments made using this spectrum.

The example above, the $N = Z - 2$ system in medium mass nuclei, probably represents the limit for spectroscopy using conventional methods with stable beams. With the advent of radioactive beams, new methodologies become available for accessing the most proton-rich systems. With ISOL beams this is achieved through pursuing fusion-evaporation reactions with radioactive beams of neutron deficient radioactive isotopes - closer to the nuclei of interest, yielding large cross sections. However, high energy fragmentation reactions probably provide the most productive method at present. One example of this is described below, where states in the $T_z = -\frac{3}{2}$ nuclei ^{49}Fe and ^{53}Ni were observed [28] for the first time using "mirrored" fragmentation reactions.

At facilities such as the National Superconducting Cyclotron Facility (NSCL) at Michigan State University or at GSI Darmstadt, high energy beams (several GeV and above) can be used to impinge on a thick Be production target to produce a wide range of relativistic exotic nuclear fragments. These are directed into mass spectrometers to select and identify exotic nuclei which are then selected as the "radioactive beam". In the example cited here, a ^{58}Ni beam of 160 MeV per nucleon energy at the NSCL facility impinged on thick Be target at the entrance of the A1900 spectrometer [29] which was tuned to provide a beam of radioactive ^{56}Ni at about 100 MeV/u with the incoming beam identified event-by-event through time-of-flight measurements. This then was directed onto the Be reaction target at the centre of the SeGA gamma-ray array [25] where the nuclei of interest are created through a second reaction - e.g. fragmentation, knockout or charge exchange. Gamma rays recorded from these nuclei are tagged with the identified A and Z of the final fragment, which were determined by the S800 spectrograph [30] downstream of the reaction target. The final nuclei were identified through time of flight (giving A/Q) and energy loss at the focal plane of the spectrograph (giving Z).

The advantages of this technique are that (a) a wide range of exotic nuclei can be produced at the final target, (b) non-yrast states are more readily populated, and (c) the high energy of the recoiling fragments makes particle identification through energy loss and time-of-flight very clean. The disadvantages for this kind of spectroscopy is that only a limited number of states are populated, it is difficult to achieve high spin, and that precision gamma-ray spectroscopy is required at $v/c \approx 0.4$, which is very challenging due to high backgrounds from atomic processes and large Doppler broadening.

The wide range of proton-rich systems populated can be seen from the S800 fragment identification plot shown in Fig. 7 following fragmentation of the secondary ^{56}Ni beam. A wide range of nuclei with $Z > N$ are produced, as can be seen by the indicated lines of constant T_z. ^{53}Ni is the uppermost nuclide in the plot on the $T_z = -\frac{3}{2}$ line. The highest "row" corresponds to Ni isotopes (56-53), the next row down corresponds to Cobalt, etc. The wide range of cleanly-identified proton-rich fragments is clearly seen. All of these have associated gamma-ray spectra recorded.

Simple gating on these nuclides in the particle identification plot will yield, following suitable Doppler correction, a "singles" spectrum of the isotope of
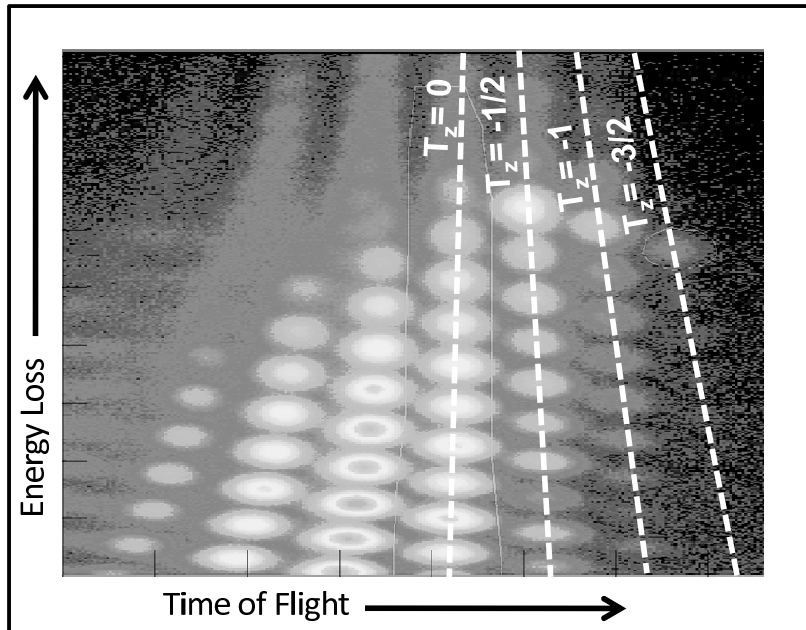
Fig. 7. The particle identification plot from the S800 from the ^{53}Ni and ^{49}Fe experiment [28]. The measurements on the axes correspond directly to Z (from energy loss) and A/Q (from time of flight) - and so each blob corresponds to a specific nuclide. The dashed lines indicate locus of constant T_z.

interest. In this experiment, to aid with the assignment of specific states to the observed gamma decays, the analogue spectra for the mirror partners were also created. This was achieved through "mirrored" fragmentation reactions. For example, ^{53}Ni – populated through the 3n removal reaction has a mirror nuclide, ^{53}Mn, populated through an analogue 3p removal from ^{56}Ni. The S800 was tuned to accept these fragments in a different setting, and in this way pairs of mirrored spectra, created through analogue reactions, were created. The example shown here is the mirror pair ^{53}Ni/^{53}Mn - populated through these mirrored reactions – see Fig. 8. This short test run was rather low on statistics, but nevertheless two excited states were observed in ^{53}Ni for the first time. The plot shows the importance, in this technique, of having the analogue spectrum present to enable the one-to-one correspondence between the states to be established visually. We will return to the significance of this result in Sect. 5.

4 Theoretical description of Coulomb Energy Differences

In the hypothesis of charge symmetry and charge independence of the nuclear force, differences in excitation energy between analogue states in mirror nuclei
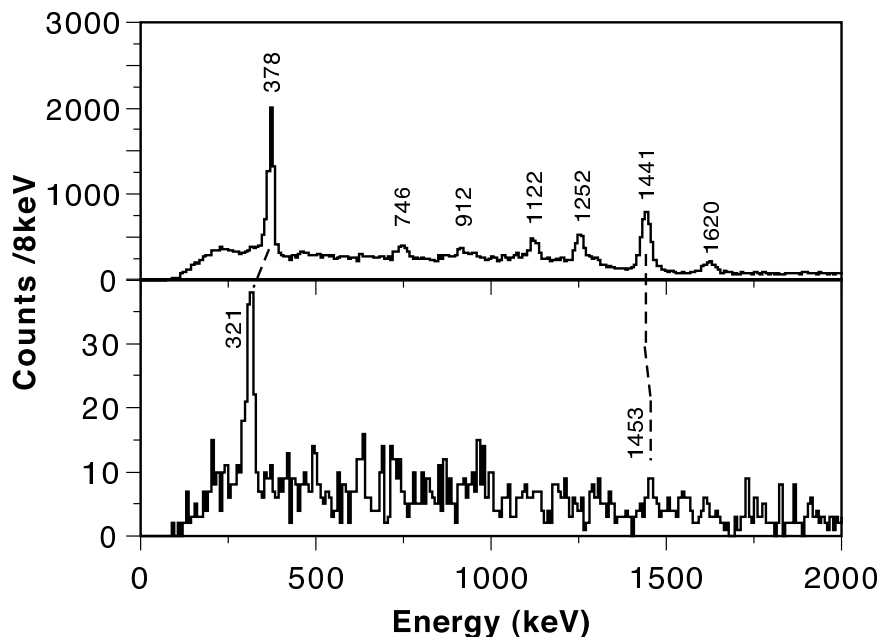
Fig. 8. The spectra for the ^{53}Ni experiment using the SeGA array at NSCL Michigan State University, selected by the S800 and populated by the three-neutron removal from ^{56}Ni. The lower spectrum is the ^{53}Ni spectrum, and the upper spectrum is the analogue spectrum populated through 3p removal from ^{56}Ni.

should be of purely electromagnetic origin. The Coulomb interaction only acts between protons, which induces an isospin dependence of the total interaction. The Coulomb field gives a contribution of the order of hundreds of MeV to the nuclear mass, and it is the Coulomb energy which plays the main role in the mass shifts between isobaric analogue states (Coulomb displacement energy (CDE), see Sect. 2.2), which are of the order of tens of MeV. Other contributions to the CDE are the difference between proton and neutron masses and other minor effects of electromagnetic character. Compared with all these contributions to the CDE, isospin breaking terms of the *nuclear* interaction are expected to be small [13].

When measuring the difference between *excited* states in isobaric multiplets, the large contributions due to the Coulomb field almost cancel out, as the ground states are normalised to zero excitation energy. Only small effects remain. In the $f_{\frac{7}{2}}$ shell, the measured energy differences between mirror nuclei (MED) amount to tens of keV and do not generally exceed 100 keV. Larger values (200-300 keV) have been encountered for some particular states in nuclei of the *sd* shell. For energy differences in $T = 1$ isobaric triplets in the $f_{\frac{7}{2}}$ shell, the measured TED values are smaller than 200 keV. Nevertheless, these rather small energy differ-

ences have demonstrated to act as a magnifying glass that highlights specific *nuclear* structure features. Moreover, if the Coulomb effects can be theoretically estimated, isospin-breaking effects due to the nuclear interaction could be revealed.

Given the small values of the mirror and triplet energy differences, it is very challenging from the theoretical point of view to get a good quantitative description. There have been pioneering calculations in the framework of the cranked shell model [31] that have given a qualitative interpretation of the first experimental results of MED in deformed nuclei in the middle of the $f_{\frac{7}{2}}$ shell. It was in the middle of the nineties when important advances in the theoretical techniques allowed to perform large scale shell model calculations that were able to reproduce for the first time the rotational spectra of these nuclei [32–34] and to allow a better description of Coulomb energy differences. This was not only due to the constant improvement in computational power but also to the development of new codes for shell model calculations [35–37]. Since then, the remarkable synergy between theoretical and experimental groups has allowed detailed studies of several physical properties of light- and medium-mass nuclei to be undertaken. The reliability of shell-model calculations in describing the spectroscopy of medium-light nuclei, and in particular those in the $f_{\frac{7}{2}}$ shell, encouraged the extension of these calculations to the description of such small energy differences as the experimental MED and TED in isobaric multiplets. This constitutes a stringent test of the calculations due to the subtle details under examination.

Three are the main ingredients of a shell model calculation. The first is the model space. *Ab initio* calculations are only possible for light nuclei, but for medium and heavy nuclei, only a certain number of levels can be considered in the calculation. An "inert" core has to be assumed, limiting the model space to some few orbitals and, in general, limiting the number of valence particles that can be excited within this space. The choice of the valence space is, therefore, limited by the capability of the computational procedure to deal with the dimension of the matrix to be diagonalised. Presently, exact large-scale shell-model calculations in the m-scheme, using the Lanczos method for the diagonalisation of the matrices, can cope with dimensions of the order of 10^{10}. This is the method used by the code ANTOINE, developed by the Strasbourg group [35,38]. Higher dimensions can be dealt with by quantum Monte Carlo techniques, such as the Monte Carlo Shell Model (MCSM) code developed by the theoretical nuclear group in Tokyo [36,39].

The second ingredient is the effective interaction valid in the chosen model space. A variety of effective interactions have been developed, and continue to be developed, to describe different mass regions in the table of isotopes. They mock up the general Hamiltonian in the restricted basis. The $f_{\frac{7}{2}}$ shell, between the doubly magic nuclei ^{40}Ca and ^{56}Ni, constitutes a very special case, as it can be considered to be an isolated shell. This simplistic approximation allows straightforward predictions to be made [40]. However, it is clear that the $1f_{\frac{7}{2}}$ shell-model space is not sufficient to describe the spectroscopy of these nuclei

with good accuracy – in particular the collective states – and that the rest of the fp orbitals, $2p_{\frac{3}{2}}$, $1f_{\frac{5}{2}}$ and $2p_{\frac{1}{2}}$, have to be taken into account in the calculations. In this respect, the most reliable interactions in the full fp valence space for the description of $f_{\frac{7}{2}}$-shell nuclei are KB3G [41] and GXPF1A [42]. The USD interaction [43,44], in the $d_{\frac{5}{2}}$,$s_{\frac{1}{2}}$,$d_{\frac{3}{2}}$ shell-model basis, gives a good description of the spectroscopy of positive-parity states of light sd-shell nuclei. An improved version, called USDB, has been recently developed by B.A. Brown [45]. Beyond the middle of the shell, however, particle-hole excitations to the fp shell become important in the configuration of natural-parity states and are absolutely necessary for constructing negative-parity states. An exact calculation in the two main shells implies a large valence space and the dimensions of the matrices to be diagonalised become extremely large. Suitable truncations of the basis are therefore needed. For the upper sd shell, an effective interaction in the reduced valence space composed by the $s_{\frac{1}{2}} d_{\frac{3}{2}} f_{\frac{7}{2}} p_{\frac{3}{2}}$ orbitals, the $sdfp$ interaction, has been introduced by Caurier and collaborators in Ref. [46]. This proves to give a good description, along the $N = Z$ line, of the spectroscopy of $A \sim 35$ nuclei such as ^{34}S [47] and ^{35}Cl [48], and for neutron-rich nuclei. Around $A = 30$, the closed shell at $N = Z = 14$ does not hold and excitations from the $d_{\frac{5}{2}}$ shell have to be considered. In these cases, the SDFP-M interaction [49] in the larger $d_{\frac{5}{2}} s_{\frac{1}{2}} d_{\frac{3}{2}} f_{\frac{7}{2}} p_{\frac{3}{2}}$ valence space can be used within the MCSM [36].

The third ingredient are the single particle energies. They are in general taken from the experimental value for the core plus one nucleon. The difference between proton and neutron single particle energies are in general ignored as they introduce, together with the Coulomb interaction, small corrections to the energy levels. When computing the Coulomb energy differences, these differences result very important and it is necessary to understand there origin.

In the next subsections we present some details on how the MED and TED are obtained in the shell-model framework for nuclei in the $f_{\frac{7}{2}}$ shell. Extensions to other mass regions can be found in the review article [50]. We describe the different contributions to the excitation energy differences, following the studies in the shell model framework by Zuker and collaborators [17,51–53]. For these calculations we have used the code ANTOINE [35]. The effective interaction used is the KB3G [41] for the fp shell.

4.1 Electromagnetic effects

The Coulomb field or, more generally, the electromagnetic interaction is the main interaction responsible for differences in excitation energy between isobaric analogue states. This interaction yields several effects on the MED and TED and depending on the nuclear structure properties of the different nuclei, some effects can be more evident than others. The possibility of having a rich quantity of good experimental data allows for a detailed study of these effects. In the next paragraphs we describe the several terms that contribute to the excitation energy differences. Following the formalism developed in Refs. [38,52], the effective shell model Hamiltonian is divided into a monopole plus a multipole component.

While the monopole part determines the single particle energies and the unperturbed energy of the different configurations, the multipole part has to do with correlations and configuration mixing.

The multipole Coulomb term: test of nucleon alignment. The role of the multipole Coulomb interaction in the MED of deformed nuclei in the middle of the $f_{\frac{7}{2}}$ shell was put in evidence for the first time by Cameron *et al.* [54]. Studying the mirror nuclei ^{49}Mn/^{49}Cr they explained the enhancement of the MED with increasing spin in terms of the *alignment* of the spins of pairs of nucleons.
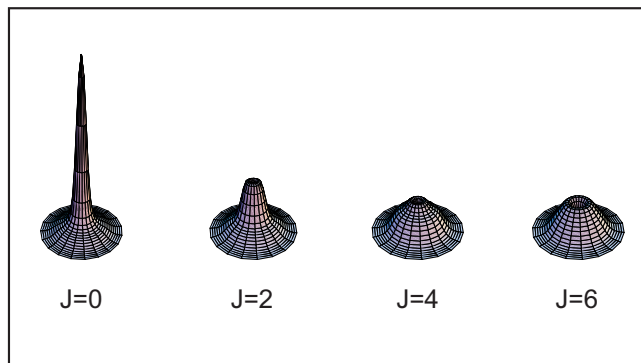
Fig. 9. A calculation of the probability distribution for the relative distance of two like-particles in the $f_{\frac{7}{2}}$ shell as a function of their coupled angular momentum. The calculations were undertaken in Ref. [55]. The centre of each plot corresponds to zero separation.

This results from the fact that the Coulomb interaction between two protons coupled in time-reversed orbits is larger than for any other coupling, as the spatial overlap of their orbits is maximum. This can be seen in Fig. 9, which shows how the average separation of two like-particles in the $f_{\frac{7}{2}}$ shell increases with their coupled angular momentum [55]. Thus, when two protons coupled to $J = 0$ re-couple their angular momenta, the Coulomb energy decreases. In particular, when a pair of protons aligns to the maximum value $(2j - 1)$ in a single j-shell, the Coulomb energy between them reaches its minimum value as their spatial separation is largest. As the Coulomb interaction is repulsive, the effect of the alignment reduces the excitation energy of the nuclear state where the alignment occurs. Of course, the alignment of any pair of nucleons along a rotational

band causes changes in the energy sequence, which is called back-bending as, in a spin vs. transition energy plot, the smooth behaviour is interrupted due to a decrease in the transition energy. This nuclear effect, however, will be equal in both mirror partners in the hypothesis of isospin symmetry of the nuclear interaction. On the other hand, only in the nucleus where the proton pair aligns will the Coulomb effect occur. Due to the isospin symmetry, in its mirror partner, a pair of *neutrons* will align at the same state – without any Coulomb effect. Thus, just by looking at the experimental MED of a rotational mirror pair, one would be able to deduce which type of nucleons are aligning at the back-bend. A significant increase (decrease) of the MED would mean that a neutron (proton) pair is aligning in the proton-rich nucleus and, consequently, a proton (neutron) pair in its mirror partner. This is schematically shown in Fig. 10.
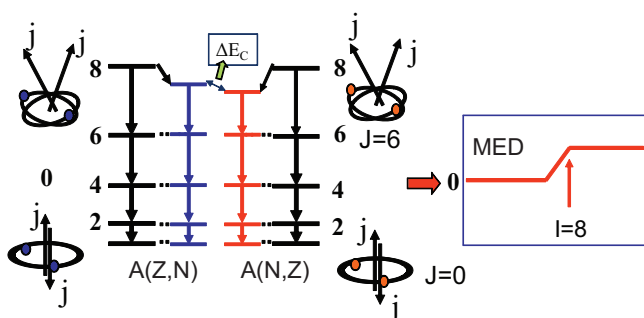
Fig. 10. Two rotational bands in mirror nuclei where a pair of neutrons in the nucleus on the left is aligning at $I = 8$ whilst a pair of protons due to the isospin symmetry is aligning in the nucleus on the right. The Coulomb effect on the latter one manifests as a "jump" on the MED.

In the schematic picture described above, it is the re-coupling of the angular momentum vectors that triggers the change in the MED. In general terms, this multipole Coulomb effect will have a large impact on the MED whenever any re-coupling of the angular momenta of a pair of protons occurs. A very clear example of this effect can be seen in the mirror pair $A = 51$ described in detail in Sect. 5.1. Another example are the mirror pair $A = 50$ reported in Fig. 11. In panel a), the MED curve for the mirror nuclei ^{50}Fe-^{50}Cr is shown in comparison with the shell model calculation where the Coulomb interaction has been added to the effective interaction (KB3G) in the fp shell. In these calculations the single particle energies for protons and neutrons have the same values, taken from the spectrum of ^{41}Ca, and the matrix elements for the Coulomb interaction have been obtained in the harmonic oscillator basis. The theoretical curve does not fit well the data but the trend is reproduced. This indicates that other ingredients are missing in the calculation of the MED but also shows that a re-coupling of neutrons (protons) in ^{50}Fe (^{50}Cr is going on up to J=8 while at J=10 the alignment of the other type of nucleons occurs.

The alignment process can be accounted for by shell-model calculations in the following way. Consider the operator $A_\pi = [(a_\pi^+ \, a_\pi^+)^{J=2j+1} \, (a_\pi \, a_\pi)^{J=2j+1}]^0$, that "counts" the number of proton pairs in a j orbital coupled to the maximum spin ($J = 2j - 1$). In the $f_{\frac{7}{2}}$ shell, $J = 6$. We can then calculate the expectation value of this operator at each excited state. Doing this for both nuclei, one can then calculate the difference $\Delta_{pp} = A_\pi(Z_>) - A_\pi(Z_<)$ for the mirror pair, as a function of the angular momentum. If the alignment of a pair of protons in the nucleus with charge $Z_>$ – and, consequently, the alignment of a pair of neutrons in the $Z_<$ – occurs first, ΔA_π will increase, whilst it will decrease if the opposite happens. This was introduced by Poves and Sánchez-Solano in Ref. [56]. The numerical results of $-\Delta_{pp}$ for the mirror pair $A = 50$ are reported in Fig. 11b). The choice of plotting the inverse (minus sign) is to compare directly with the Multipole Coulomb contribution to the MED. The two curves have a very similar behaviour and the interpretation of the MED changes as a function of the angular momentum can be clearly deduced.
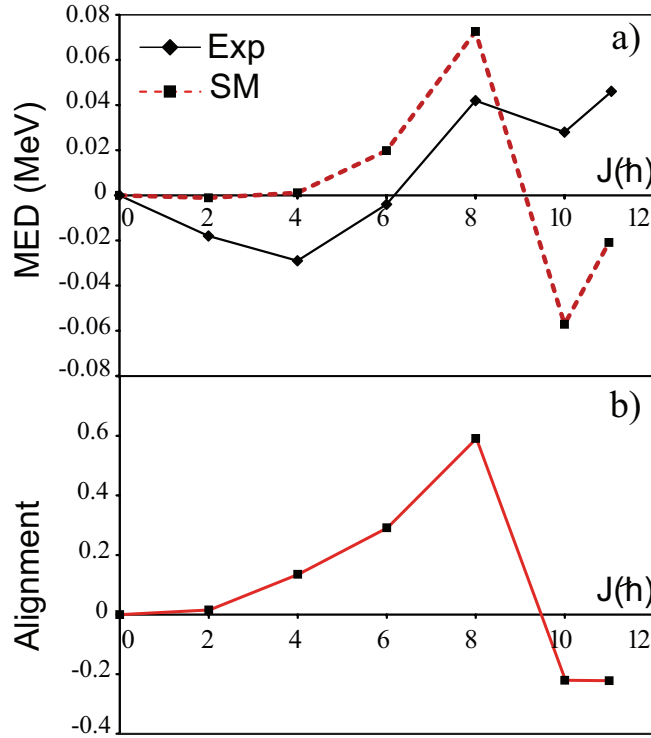
Fig. 11. a) Experimental MED and the Multipole Coulomb effect for the mirror pair ^{50}Fe-^{50}Cr; b) shell model calculation of the "alignment". See text for details

The monopole Coulomb contributions: shape changes and single-particle energies. As discussed above, to get a good quantitative description of the experimental MED other terms are required in the calculation of the MED. In particular, an important contribution to the comprehension of the origin of the MED was given, for the first time, in Ref. [51] for the case of the $A = 50$ mirror pair of Fig. 11. It was pointed out that, in addition to the multipole Coulomb interaction between valence protons, there was a small but significant *monopole* Coulomb effect due to the change of the nuclear radius along the rotational band.

In a rotational band, the mechanism of generating angular momentum by aligning the valence-particle spins in a high-j orbit becomes energetically favoured with increasing rotational frequency. In $f_{\frac{7}{2}}$-shell nuclei, the occupation of orbits different from the $f_{\frac{7}{2}}$, important to create collective states near the ground state, decrease along the rotational bands producing changes of the nuclear radius. This affects the MED as valence protons in orbitals with smaller radii are nearer to the charged core and have more Coulomb energy.

Following Refs. [51,52], the monopole Coulomb contribution to the MED can be deduced by considering the Coulomb energy of a uniformly charged sphere of radius R_C

$$E_C = \frac{3}{5} \frac{Z(Z-1)e^2}{R_C} \tag{13}$$

The difference between the energy of the ground states of $T_z = \pm\frac{k}{2}$ mirror nuclei ($Z_> = Z_< + k, Z = Z_>$) is

$$\Delta E_C = E_C(Z_>) - E_C(Z_<) \simeq \frac{3}{5} \frac{k(2Z-k)e^2}{R_C}. \tag{14}$$

This energy difference amounts to tens of MeV and is the main ingredient in the evaluation of CDE (see Sect. 2.2 and Ref. [17]). When calculating the mirror energy differences for each state of spin J as a function of the angular momentum, we refer the MED(J) values to the ground state. On doing so, the monopole effect of ΔE_C almost vanishes. A small contribution remains, however, due to the change in charge radius with the angular momentum, as discussed above. The monopole Coulomb radial contribution to the MED can thus be written:

$$\Delta_M <V_{Cr}(J)> = \Delta E_C(J) - \Delta E_C(0) = -\frac{3}{5}k(2Z-k)e^2\frac{\Delta R(J)}{R_C^2} \tag{15}$$

where Δ_M is the MED and $\Delta R(J) = R_C(J) - R_C(0)$ and we assume, following Refs. [17,51,52], that it is the same in both mirror nuclei.

Nuclei that lie near the middle of the $f_{\frac{7}{2}}$ shell are well deformed at low spin. These states are more collective than the high-spin members of the rotational band and the wave functions have an important contribution of the $p_{\frac{3}{2}}$ orbit. In fact, it is the coupling between the $f_{\frac{7}{2}}$ and the $p_{\frac{3}{2}}$ orbits what gives rise to the quadrupole collectivity in this mass region [57]. With increasing angular

momentum, the yrast bands evolve by progressively aligning the valence nucleons in the $f_{\frac{7}{2}}$ shell up to the band terminating state. On doing that, the occupation of the $p_{\frac{3}{2}}$ orbit decreases and the bands terminate in non-collective, high-spin states with all the valence particles in the $f_{\frac{7}{2}}$ shell. The role of the other orbits, $f_{\frac{5}{2}}$ and $p_{\frac{1}{2}}$, is less important, and does not change very much as a function of the angular momentum.

In the fp shell, p-orbits have larger radius than f-orbits and therefore, the Coulomb repulsion increases as the protons pass from the $p_{\frac{3}{2}}$ to the $f_{\frac{7}{2}}$ orbit. In other words, at high spin, when all nucleons are filling the $f_{\frac{7}{2}}$ shell, the monopole Coulomb contribution is larger than at low spin, where there is a significant $p_{\frac{3}{2}}$ contribution to the wavefunction. How to account for this effect in the shell-model framework will be discussed in Sect. 4.3, together with the other terms. It is important to note that the effect of the change of deformation in the MED was also introduced in Ref. [58] and calculated within the Liquid Drop model.

The monopole term of the Coulomb interaction has also an effect on the single-particle energies. It modifies not only the energy of the protons but also that of the neutrons, in different ways [13,17]. In Ref. [17], Duflo and Zuker show that the contribution of the monopole Coulomb interaction to the CDE can be expressed as the energy of a charged sphere (Eq. (13)) with single-particle corrections that account for shell effects. They affect the energy of the proton orbits proportionally to the square of the orbital momentum l in the harmonic oscillator representation. The expression for the single-particle splittings for a proton in a main shell, with principal quantum number N, above closed shell Z_{cs} results [17]

$$E_{ll} = \frac{-4.5 Z_{cs}^{13/12}[2l(l+1) - N(N+3)]}{A^{1/3}(N + \frac{3}{2})} keV. \qquad (16)$$

The effect on the single-particle energies is sizable. In ^{41}Sc (Z_{cs}=20, N=3), proton f orbits are lowered by $\sim$45 keV while the energy of p orbits is raised by $\sim$105 keV with respect to the neutron levels. The relative energy between the proton $f_{\frac{7}{2}}$ and $p_{\frac{3}{2}}$ orbitals is therefore increased by $\sim$150 keV with respect to the neutron energy difference.

Another interaction that affects the single-particle energies is the relativistic *electromagnetic* spin-orbit force (EMSO) [13,59]. This interaction, analogous to the atomic case, results from the Larmor precession of the nucleons in the nuclear electric field due to their intrinsic magnetic moments and to the Thomas precession experienced by the protons because of their charge. The effect of the *nuclear* spin-orbit hamiltonian in the single-particle spectrum is very well known. It amounts to several MeV and acts on both protons and neutrons. The EMSO effect is about 50 times smaller than the nuclear spin-orbit potential and has been in general ignored in MED calculations. However, as it acts differently on neutrons than on protons, its effect does not cancel when computing MED values and can become very important for some particular states [60,53].

The general expression of the electromagnetic spin-orbit potential [13,59] is:

$$V_{ls} = (g_s - g_l)\frac{1}{2m_N^2 c^2}(\frac{1}{r}\frac{dV_C}{dr})\boldsymbol{l} \cdot \boldsymbol{s}, \tag{17}$$

where g_s and g_l are the gyromagnetic factors, V_C is the Coulomb potential and m_N is the nucleon mass. The term proportional to g_s is the Larmor term. It can be deduced by considering the potential energy of a spin magnetic moment μ_s in an effective magnetic field due to its motion in the electric field generated by the protons in the nucleus. The second term in Eq. (17), proportional to g_l, is the relativistic Thomas term associated with the orbital magnetic moment μ_l, that vanishes in the neutron case.

To have a rough estimate of the energy shift produced by the relativistic electromagnetic spin-orbit term we assume that the Coulomb potential is generated by a uniformly charged sphere of radius R_C [13]

$$E_{ls} \simeq (g_s - g_l)\frac{1}{2m_N^2 c^2}(-\frac{Ze^2}{R_C^3})\langle \boldsymbol{l} \cdot \boldsymbol{s} \rangle. \tag{18}$$

Using for example the free values of the gyromagnetic factors $g_s^\pi = 5.586$, $g_l^\pi = 1$ and $g_s^\nu = -3.828$, $g_l^\nu = 0$ for the proton and the neutron, respectively, it is easy to see that the energy shift will have different sign for a proton orbit than for a neutron one. The sign will also depend on the spin-orbit coupling, as $\langle \boldsymbol{l} \cdot \boldsymbol{s} \rangle = l/2$ when $j = l + s$ and $\langle \boldsymbol{l} \cdot \boldsymbol{s} \rangle = -(l+1)/2$ when $j = l - s$. When considering, for example the $f_{\frac{7}{2}}$ and the $d_{\frac{3}{2}}$ which are involved in excited states of nuclei in the upper sd shell. The effect of the EMSO is to reduce the energy gap between the proton orbitals by $\sim$120 keV and to increase it for neutrons by roughly the same amount. Therefore, in one nucleus the energy of a state whose configuration involves the excitation of one proton from the $d_{\frac{3}{2}}$ to the $f_{\frac{7}{2}}$ will be smaller than that of the analogue state in its mirror nucleus where a neutron undergoes the excitation. The MED for such states will reach large values. On the contrary, small MED will be obtained whenever the configuration of the state involves the excitation of one proton *or* one neutron with similar probabilities, as the effect is compensated. The negative parity bands in the mirror nuclei ^{35}Ar-^{35}Cl are a good example of the effect of the electromagnetic spin orbit on the MED, where large values (about 300 keV) have been measured for several states.

4.2   A new isospin-breaking term

Taking into account the different Coulomb terms introduced in the previous sections in the calculation of the MED, the theoretical curves do allow still a good quantitative agreement with data. This can be seen, for example, in Fig. 12, where the MED for the rotational bands in the mirror pair ^{49}Mn-^{49}Cr are displayed in comparison with the calculations. In ref. [51] a renormalization of the Coulomb interaction in the fp shell was proposed to improve the description. However, it was seen that a single renormalization could not account for all the available data in the $f_{\frac{7}{2}}$ shell. A satisfactory solution was then proposed by
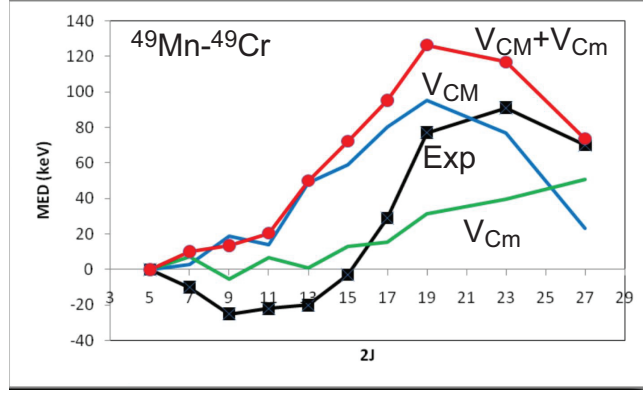
Fig. 12. MED for the mirror pair ^{49}Mn-^{49}Cr. The addition of the monopole (V_{Cm}) and the multipole Coulomb (V_{CM}) contributions give rise to a theoretical curve that is compared to the experimenatl MED (Exp).

Zuker, as described in Ref. [52]. Analysing the data for the $A = 42$ isobaric triplet, it was shown that the MED and TED values could not be reproduced by just considering the electromagnetic interaction and an additional isospin non-conserving term was thus called into play [52].

Let us consider the yrast states $J = 0, 2, 4, 6; T = 1$ in the three isobaric nuclei ^{42}Ti, ^{42}Sc and ^{42}Ca and assume that they have essentially $f_{\frac{7}{2}}^2$ configurations. In this hypothesis, a two-body effective interaction in the $f_{\frac{7}{2}}$ shell can be obtained from the experimental data. In fact, the isovector term of the interaction can be deduced from the MED whilst the TED give the isotensor component as follows,

$$MED_J(A = 42, T = 1) = V_{CM,f_{\frac{7}{2}}}^{(1)}(J) + V_{B,f_{\frac{7}{2}}}^{(1)}(J)$$

$$TED_J(A = 42, T = 1) = V_{CM,f_{\frac{7}{2}}}^{(2)}(J) + V_{B,f_{\frac{7}{2}}}^{(2)}(J), \qquad (19)$$

where an isospin symmetry breaking V_B term is considered, in addition to the Coulomb component. Here, we consider only the multipole Coulomb term, as no changes in deformation are expected along the yrast sequence. The multipole Coulomb term can be calculated for two protons in the $f_{\frac{7}{2}}$ shell. By subtracting this term from the MED and TED data in Eq. (19), we would expect that, in the hypothesis of isospin symmetry and independence respectively, the contribution of $V_{B,f_{\frac{7}{2}}}^{(1)}$ and $V_{B,f_{\frac{7}{2}}}^{(2)}$ for all J values should be negligible.

This is not at all the case. Large differences are found which means that the isospin symmetry breaking V_B term cannot be ignored in the calculation of the excitation energy differences. The larger differences are found in the TED at $J = 0$ for the while for the isovector (MED) components the peak is obtained for two $f_{\frac{7}{2}}$ nucleons coupled to $J = 2$. This effect was already noted in early

studies performed by Brown and Sherr in Ref. [61] but the origin of this charge-dependent interaction is still an open question.

We do not enter into details now on the deduction of the V_B term, a complete discussion can be found in Ref. [52]. A very schematic and simple ansatz was proposed in Ref. [52] that consists on constructing an isospin breaking interaction (ISB) in the fp shell by just taking one $f_{\frac{7}{2}}^2$ matrix element with a strength determined by the data for $A = 42$.

$$V_{B,fp}^{(1)} = \beta_1 V_{B,f_{\frac{7}{2}}}(J = 2)$$
$$V_{B,fp}^{(2)} = \beta_2 V_{B,f_{\frac{7}{2}}}(J = 0) \tag{20}$$

where $V_{B,f_{\frac{7}{2}}}(J)$ are matrix elements with unit value. The choice of $V_{B,f_{\frac{7}{2}}}(J = 2)$ for the isovector and $V_{B,f_{\frac{7}{2}}}(J = 0)$ for the isotensor components is based on the leading terms (see ref. [52,50]). In Ref. [52], the strengths used were $\beta_1 = \beta_2 = 100$ keV. These schematic interaction showed to be essential to describe all the MED and TED hitherto known in the $f_{\frac{7}{2}}$ shell, without changing the strength [50]. To illustrate this with an example, we can see in Fig. 13, that the experimental curve is now very well described by the theory when the V_B term is added to the electromagnetic contributions. It is interesting to note that the ISB contribution to the MED in mass $A = 49$ is of the same magnitude of the others, a fact that was in principle unexpected, under the assumption of charge symmetry of the effective interaction.
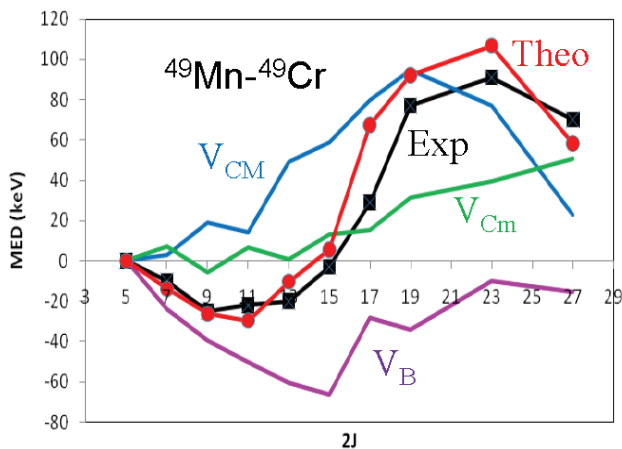
Fig. 13. MED for the mirror pair ^{49}Mn-^{49}Cr. The addition of the calculated monopole (V_{Cm}), the multipole Coulomb (V_{CM}) and the ISB (V_B) contributions give rise to a theoretical curve (SM) that compares very well with the experimental MED (Exp).

4.3   Calculation of MED and TED

Taking into account the different contributions described above to the MED and TED, monopole and multipole Coulomb and the ISB terms, can be written as,

$$MED(J) = \Delta_M < V_{CM}^J + V_{Cm}^J + V_B^{(1,J)} > \qquad (21)$$

$$TED(J) \ = \Delta_T < V_{CM}^J + V_B^{(2,J)} > \qquad (22)$$

where Δ_M means the difference between the mirror nuclei (Eq. (11)) and Δ_T stands for the difference in the triplet (Eq. 12). The brackets indicate that we can rely on the fact that isospin non-conserving effects are small and therefore they can be treated in first order perturbation theory. We can thus perform a diagonalisation of the nuclear effective interaction and calculate the contribution of the different terms by means of the expectation values.

The calculation of the contributions of the multipole Coulomb and the V_B terms is straightforward. The effect of the modification of the single-particle energies can also be obtained by considering different energies for the protons and the neutrons following the formulas introduced above. Finally, changes in the charge radius can be accounted for, within the shell model, by considering the evolution of the occupation numbers of the different orbits as a function of the angular momentum along the yrast bands [51]. For nuclei in the $f_{\frac{7}{2}}$ shell, it is the relative occupation of the $p_{\frac{3}{2}}$ orbit which determines the main changes of radii. The assumption of equal radii of the mirror partners means that a calculation of the *average* of proton and neutron occupation numbers of the $p_{\frac{3}{2}}$, m_π and m_ν, respectively, is required: $\frac{m_\pi + m_\nu}{2}$. The contribution of the monopole Coulomb radial term to the MED of mirror nuclei with $|T_z| = k/2$ can be parameterised as,

$$\Delta_M < V_{Cm}^J > = k \ \alpha_r \left(\frac{m_\pi(0) + m_\nu(0)}{2} - \frac{m_\pi(J) + m_\nu(J)}{2}\right) \qquad (23)$$

where the constant α_r can be deduced from the data in mass $A = 41$. In the $f_{\frac{7}{2}}$ shell the value adopted is 200 keV.

It is important to note that the radial term in the calculation of the MED is not a single-particle effect and therefore it cannot be accounted for by setting different single-particle energies for protons and neutrons in the shell-model calculation. The radial contribution vanishes in the calculation of the TED [52]. Monopole Coulomb single-particle contributions to the MED are proportional to the *difference* between the proton and the neutron occupation numbers. This difference is small in most of the $T_z = \pm\frac{1}{2}$ and $T_z = \pm 1$ mirror nuclei studied in the $f_{\frac{7}{2}}$ shell. On the other hand, for nuclei in the upper sd shell, the promotion of nucleons to the fp shell becomes important already at low spin and excitation energy. In these cases, the difference of occupation numbers between protons and neutrons are significant and single-particle Coulomb effects can become important.

5   Case Studies: The MED components in action

In this section we consider the effects of the terms identified in the calculation of MED and TED and described in Sect. 4.1, 4.2 and 4.3. We cite individual examples where the effects are clearly present and where they make a key contribution. It should be noted that the consistent calculations presented here are all calculated the same way - no effects are "switched off". However, it is observed that the various terms can have a lesser or greater importance depending on location in the shell. For example, it is seen that the C_m term tends to be more pronounced in the middle of the $f_{\frac{7}{2}}$ shell and has a lesser effect when the shell gaps are approached. However, it is always included.

5.1   The Multipole Coulomb interaction at work: the mirror pair ^{51}Mn-^{51}Fe

The multipole term, C_M is associated with the recoupling of angular momenta of pairs of nucleons. Generally, this re-coupling occurs gradually as a function of increasing spin as we increase excitation energy and angular momentum, although occasionally a sudden re-coupling occurs. When a pair of protons have their angular momentum vectors realigned (say from $J = 0$ to the maximally aligned (for $f_{\frac{7}{2}}$ shell) value of $J = 6$), there is a reduction of their overlap and a concomitant reduction in the Coulomb energy of the pair. As there is no Coulomb effect for pairs of neutrons, this means that although the binding energy of both proton and neutron pairs decreases with increasing alignment, the binding energy of the pair decreases *less* for protons than for neutrons. The difference is about 100 keV for a full recoupling in the $f_{\frac{7}{2}}$ shell) and this appears clearly in the MED. This effect was first noted by Cameron *et al.* [54] and has been used in the interpretation of MED ever since [50].

The Coulomb multipole effect is always important when considering the progression of MED with increasing spin, although it is not always dominant. A good example to show the effect is the ^{51}Mn-^{51}Fe mirror pair, the MED for which are shown in Fig. 14. In Fig. 14(a) the experimental MED can be compared with the total shell-model calculation using the complete prescription described earlier. The agreement between the experiment and model is spectacularly good. The main trends of the MED were discussed in Bentley *et al.* [56] and Ekman *et al.* [62] and explained in terms of the multipole component C_M. The main feature is the sudden dip in the MED at $J^{\pi} = \frac{17}{2}^{-}$ followed by a rise as the band termination at $J^{\pi} = \frac{27}{2}^{-}$ is approached. The $J^{\pi} = \frac{17}{2}^{-}$ state in ^{51}Fe is interpreted as a pair of $f_{\frac{7}{2}}$ protons coupled to the maximum $J = 6$ coupled to the $J^{\pi} = \frac{5}{2}^{-}$ ground state. As the re-coupling occurs, the Coulomb energy of the pair of protons reduces. In ^{51}Mn the re-coupling occurs, instead, with neutrons – with no such Coulomb effect of course. The net effect is that states associated the proton alignment become more strongly bound than their analogue states - hence the negative MED. Beyond $J^{\pi} = \frac{17}{2}^{-}$ in ^{51}Fe, the proton valence space is maximally aligned, and so any further angular momentum must be generated
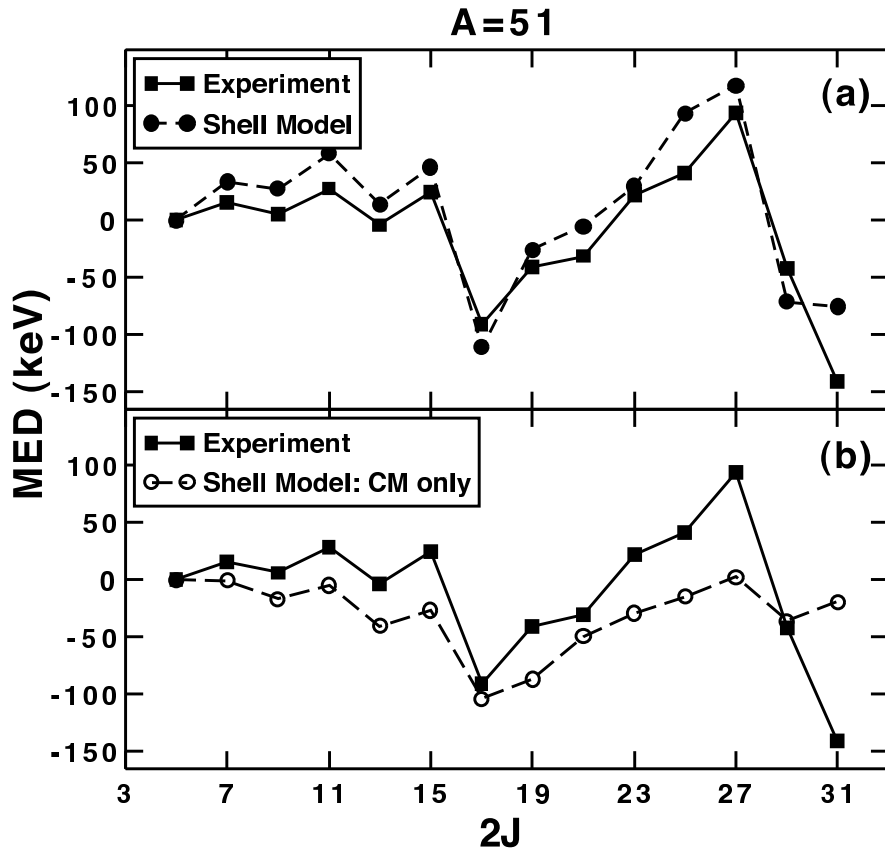
Fig. 14. The calculated and experimental mirror energy differences for the ^{51}Mn-^{51}Fe $T = \frac{1}{2}$ mirror pair. (a) The experimental [56,62] and calculated MED - see text for details. The lower panel (b) shows a comparison of the experimental data with just the C_M (Coulomb multipole) component of the calculations.

by re-coupling of neutrons (hence protons in ^{51}Mn). Thus, the MED effect must reverse and head towards zero at the band termination. This interpretation was confirmed [56] through calculations of the "alignment" as described in Sect. 4.1 and Fig. 11 – it was observed that the major trends in the MED correlated well with the calculated quasi-alignment effects.

Fig. 14(b) shows the comparison of the experimental data with just the Coulomb multipole (C_M) term. It is clear that the major trends of the MED are very well described in trend, although it is obvious that the other terms help to bring the calculations more in line with experiment.

5.2   The Monopole Coulomb interaction at work: the mirror pair ^{48}Mn-^{48}V

Monopole Coulomb contributions to the MED are of two types, as discussed in Sect. 4. The radial term, associated to changes in the charge radius as a function of the angular momentum, and the single-particle energy shifts due to the electromagnetic spin-orbit and orbital terms. As stated in Sect. 4, changes in the single-particle energies have an impact in the MED only when the configuration of the state involves a pure single particle spin-flip excitation. This is not the case in most of the nuclei studied in the $f_{\frac{7}{2}}$, except in very few cases. The mirror pair we choose to illustrate the monopole effects, is one of these cases. We will first concentrate on the radial term and come to the single-particle effects below.
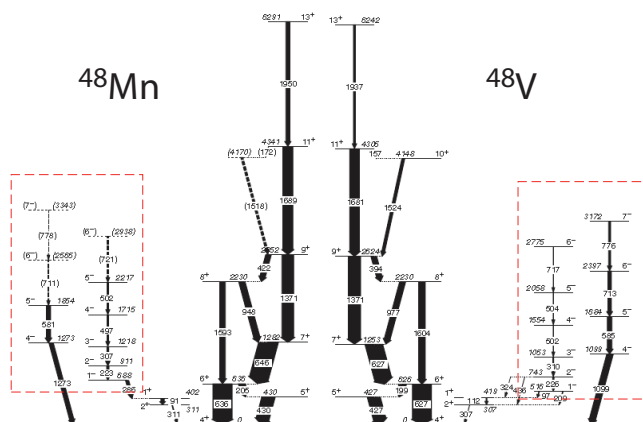
Fig. 15. The level schemes of the mirror nuclei ^{48}Mn and ^{48}V. Data from Ref. [27]

The effect of the radial term is put in evidence in a spectacular way in the odd-odd $T = 1$ mirror pair, ^{48}Mn/^{48}V [27]. This is due to two main reasons. The first one is that these nuclei lie in the middle of the shell and therefore can develop a sizable deformation. Alignment of nucleons along the yrast bands will make the occupation of the $p_{\frac{3}{2}}$ orbital decrease and so the radius. The second effect is that multipole effects such as the multipole Coulomb and the ISB terms almost completely cancel out in the MED. In fact, in a pure $f_{\frac{7}{2}}$ valence space, then both ^{48}Mn and ^{48}V have three active valence protons (holes and particles respectively) and three active valence neutrons (particles and holes respectively). As a result the contribution of the multipole terms in each nucleus must be identical. Thus, even though a pure $f_{\frac{7}{2}}$ structure is unrealistic, we still expect the (usually dominant) multipole contributions to the MED variations to be much reduced. This is seen clearly in the multipole components of the model (C_M and V_B – see Fig. 16(b)) which are small and, in fact, of the opposite sign

to the trend of the data in Fig. 16(a). The monopole effect we consider here (C_m) is clearly the remaining dominant component.
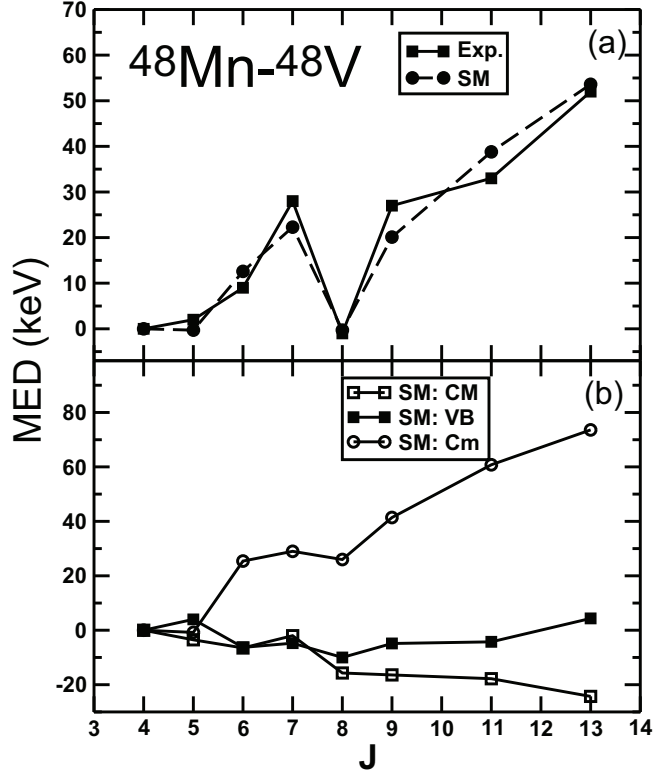
Fig. 16. The experimental (Exp.) and predicted (SM) MED for the odd-odd $T_z = \pm 1$, $A = 48$ mirror pair. In the lower panel the single contributions to the theoretical curve.

From the figure, it is clear that the C_m term steadily increases with spin because the occupancy of the $p_{\frac{3}{2}}$ orbit decreases with spin causing the reduction of the effective nuclear radius. This has the effect of increasing the Coulomb energy for *both* members of the pair, but by *more* for the $T_z = +1$ member of the pair due to the larger Z. A rise in the MED is therefore observed. This rise is almost entirely associated with the monopole radial effect.

In Fig. 15, two negative parity bands are shown for both mirror partners. From shell model calculations, these states result to be formed by a nucleon excitation from the $d_{\frac{3}{2}}$ to the $f_{\frac{7}{2}}$ orbitals. These two bands are more deformed than the ground state band. We can interpret the data in the framework of the Nilsson Model, where the $f_{\frac{7}{2}}$ odd particle and the $d_{\frac{3}{2}}$ hole can couple together to give states with $J^\pi = 1^-$ and $J^\pi = 4^-$. While these excitations in ^{48}Mn

involve a neutron excitation, a proton will excite in ^{48}V. For such a single-particle excitation, as expected, a large, positive MED is observed, of the order of 170 keV. The value is stable for all the observed states, indicating that the intrinsic structure of the states remains mainly unchanged. The largest contribution arises from the electromagnetic spin-orbit term E_{ls}, that reduces the proton gap by $\sim$ 220 keV (in a schematic calculation) with respect to the neutron gap. The orbital E_{ll} contribution does not significantly change the results in the present cases. Its effect on the proton single-particle energies is to further reduce the gap between the $f_{\frac{7}{2}}$ and the $d_{\frac{3}{2}}$ by $\sim$ 30 keV. These estimates agree well with observed MED for the two negative parity bands, indicating, just from the observed values the single-particle character of the wave functions configurations.

5.3 The isospin-breaking term at work: the mirror pairs ^{53}Co-^{53}Fe and ^{53}Ni-^{53}Mn

The isospin non-conserving term (V_B) described in Sect. 4.2 turns out to be important in many cases across the whole shell [50]. The effect can be considered as an additional repulsive isovector matrix element added to pairs of protons coupled to $J = 2$ (or an attractive component for neutrons). Naturally, as this corresponds to a low-spin coupling, the effect tends to be more important (or at least more obvious) at lower spins. This is seen, for example in Fig. 13 in Sect. 4.1 where it is clear for the $A = 49$ mirrors that the low-spin behaviour of the MED is completely inexplicable without the inclusion of the V_B term. It is also, not surprisingly, important where only a few valence particles or holes are involved in the major components of the configurations – where the low spins states near the ground states are likely to have large components of $J = 2$ of one type of nucleon. An obvious case where the effect would be expected to be significant is the $A = 54$ mirror pair where the structures are dominated by two-neutron hole or two-proton hole configurations. The work of Gadea *et al.*[63] and Rudolph *et al.* [64] showed that the effect was indeed important in the $J^\pi = 2^+$ states, and also for the states involing cross-shell excitations at higher spins [64].

   The examples chosen here are the $A = 53$ $T_z = \pm\frac{1}{2}$ mirror pair ^{53}Co-^{53}Fe [65] and the $A = 53$ $T_z = \pm\frac{3}{2}$ mirror pair ^{53}Mn-^{53}Ni [28]. The ^{53}Co-^{53}Fe pair were studied by Williams *et al.* [65] using the Gammasphere array at the Argonne National Laboratory. The ^{53}Mn-^{53}Ni pair was studied by Brown *et al.* using a two-step fragmentation reaction and the National Superconducting Cyclotron Laboratory, Michigan State University. The latter results from the analysis of the technique described in Sect. 3 and the data presented in the spectrum in Fig. 8. In Fig. 17(a) we present the MED data for the $T_z = \pm\frac{1}{2}$ pair and the full shell-model result. Again the agreement is excellent. The interpretation of the MED trend here is straightforward [65] – in ^{53}Fe ($Z = 26, N = 27$) the angular momentum is generated through a gradual re-coupling of the single pair of proton holes - neutron holes in ^{53}Co. The MED reflects this trend well with a gradual MED rise. In Fig. 17(b) we show the effect of the same calculation without the V_B term included. Here we see that the exclusion of the V_B term significantly worsens the agreement at low spin – and for the $J^\pi = \frac{9}{2}^-$ and
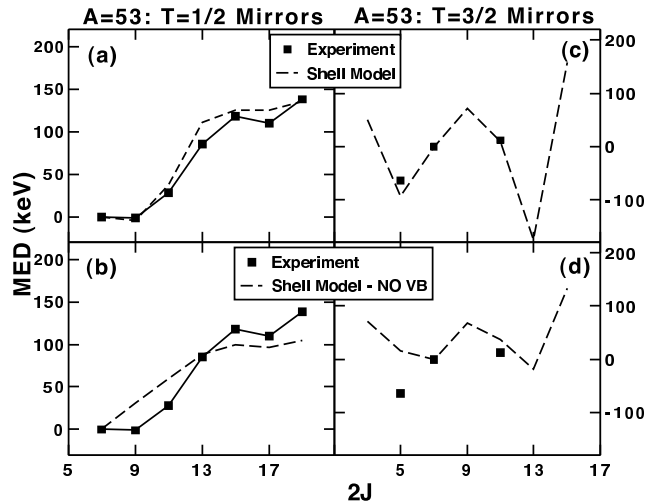
Fig. 17. (a) The experimental data for the $A = 53$ $T_z = \pm\frac{1}{2}$ mirror pair [65] compared with the full shell model calculations. (b) the same data as (a), but compared with the shell-model calculation withe V_B term removed. (c) and (d) – the same as (a) and (b) but for the $A = 53$ $T_z = \pm\frac{3}{2}$ mirror pair [28]

$\frac{11}{2}^{-}$ states in particular which might be expected to have (for ^{53}Fe) a dominant configuration based on a $J = 2$ proton-hole coupling added to the $J^{\pi} = \frac{7}{2}^{-}$ ground state. The opposite configuration applies to ^{53}Co. The large component of $J = 2$ in these low spin states makes the V_B term crucial here.

Fig. 17(c) shows the results from the $A = 53$ $T_z = \pm\frac{3}{2}$ mirror pair ^{53}Mn-^{53}Ni [28]. Only a few states were accessible experimentally here - but again the agreement is impressive for the two states where the MED has been confidently determined. Fig. 17(d) shows again the result of the calculation without the V_B term. Here, although the $J^{\pi} = \frac{11}{2}^{-}$ state is well described, the calculation fails completely for the $J^{\pi} = \frac{5}{2}^{-}$ state.

The remarkable feature about this term is that it is prevalent across the entire shell - no cases have been seen where the inclusion of this term is not necessary or where it worsens the agreement with the data (see [50]). It is also noteworthy that the effect is equally important in the deformed region in the mid-shell region, as it is in the upper and lower ends of the $f_{\frac{7}{2}}$ shell. This in turn implies that the effect is a systematic physical phenomenon that cannot be easily explained away by a failing of the shell-model prescription.

6   Conclusions and outlook

In these lectures we have shown that the study of energy differences between analogue states can give valuable information on different nuclear structure prop-

erties of these nuclei. They provide a level of consistency in detail that might seem surprising, given the long standing issues regarding modelling of Coulomb effects in nuclei (e.g. the Nolen-Schiffer anomaly). We have concentrated much of the discussion on the $f_{\frac{7}{2}}$ shell, where the Coulomb energy differences can be followed up to high-spin states and interpreted by means of state-of-the-art shell-model calculations. These studies have now developed into a mature field, and the systematic investigation of energy differences between analogue states is starting to yield some fascinating questions – such as the $J = 2$ anomaly.

In this contribution, we have concentrated on energy differences as a test of isospin symmetry. As a result, some other important aspects of isospin symmetry of isobaric multiplets have not been discussed. For example, subtle information on the isospin degree of freedom can be derived through the study of the T_z-dependence of electromagnetic transition matrix elements (see, for example, Refs. [66,67] for the $f_{\frac{7}{2}}$ shell). Mirror nuclei also provide an ideal laboratory for measurement of effective charges, as lifetimes of analogue states can be accurately determined - see for example the work of Du Reitz $et\ al.$ [67] where, information on isoscalar and isovector effective charges has been deduced from the lifetimes in the $A = 51$ mirror pair ^{51}Fe/^{51}Mn. Another key result relates to E1 decays in mirror nuclei. Because E1 decays are purely isovector in origin, in the limit of good isospin symmetry, $\Delta T = 0$ E1 transition strengths in mirror nuclei should be identical - i.e. have identical strengths. However, it now appears that E1 transitions have shown some anomalous results. For example, in the $A = 35$ [53,68], $A = 31$ [69,70] and $A = 45$ [71] mirror nuclei, strong E1 decays have been observed from certain states in one member of the mirror pair, which are either absent, or highly hindered, in the other. Recently, different E1 strengths have been determined in the mirror pair ^{67}As-^{67}Se [72]. The breakdown of the isospin selection rule has been interpreted in terms of isospin mixing [53,72].

The development and availability of the first generation of radioactive beam facilities has allowed for further access to exotic nuclei. These, and the planned next generation of ISOL and fragmentation facilities, will open up unprecedented access to proton-rich nuclei. As we proceed towards spectroscopic study of proton-rich nuclei of both larger isospin and heavier mass, one may expect other effects to come into play. For example, the assumption has been made so far that the wave functions of the analogue states are essentially identical. When the analogue states of interest in the proton-rich member of the multiplet are weakly bound, this is no longer expected to be the case, and some part of the energy difference observed will be due to the different spatial distributions of the analogue wave functions. This shift, the Thomas-Ehrman shift [73,74], will become more significant as the proton-rich states become more weakly bound.

Exploration of the isospin degree of freedom is certain to be one of the key nuclear-structure objectives of the new generation of radioactive beam facilities.

7   Acknowledgements

References

1. J. Jänecke in *Isospin in Nuclear Physics*, Ed. D.H. Wilkinson, North Holland, Amsterdam, 1969.
2. R. Machleidt and H. Muther, Phys. Rev. C **63** 034005 (2001)
3. G.Q. Li and R. Machleidt, Phys. Rev. C **58** 1393 (1998)
4. González-Trotter *et al.*, Phys. Rev. Lett. **83** 3788 (1999)
5. E.P. Wigner, Proceedings of the Robert A Welch Conference on Chemical Research (Robert A Welch Foundation, Houston, Texas) **1** (1957) 67
6. W. Benenson and E. Kashy, Rev. Mod. Phys. **51** 527 (1979)
7. W.E. Ormand, Phys. Rev. C **55** 2407 (1997)
8. W.E. Ormand and B.A. Brown, Nucl. Phys. A **491** 1 (1989)
9. N. Auerbach, Phys. Rep. **98** 273 (1983)
10. J. Britz, A. Pape and M.S. Anthony, At. Nuc. Dat. Tab. **69** 125 (1998)
11. A. Kankainen *et al.*, Phys. Rev. C **82** 052501(R) (2010)
12. H.A. Bethe and R.F. Bacher, Rev. Mod. Phys. **8** 82 (1936)
13. J.A. Nolen and J.P. Schiffer, Ann. Rev. Nucl. Sci **19** 471 (1969)
14. S.Shlomo Rep. Prog. Phys. **41** 66 (1978)
15. G.A. Miller, Chin. J. Phys. **32** 1075 (1994)
16. M.H. Shahnas *et al.*, Phys. Rev. C **50** 2346 (1994)
17. J. Duflo and A.P. Zuker, Phys. Rev. C **66** 051304(R) (2002)
18. I.Y. Lee, M.A. Delaplanque and K. Vetter, Rep. Prog. Phys. **66** 1095 (2003)
19. I.Y. Lee, Nucl. Phys. A **520** 641c (1990)
20. F.A. Beck, Prog. Part. Nucl. Phys **28** 443 (1992)
21. J. Simpson, Z. Phys. A **358** 139 (1997)
22. C. Rossi Alvarez, Nucl. Phys. News **3** 3 (1993)
23. F.Azaiez and W.Korten. Nuclear Physics News volume 7, number 4 (1997) 21
24. H.J. Wollesheim *et al.* Nucl. Instrum. Meth. Phys. Res. A **204** 678 (2003)
25. W.F. Mueller *et al.* Nucl. Instrum. Meth. Phys. Res. A **466** 492 (2001)
26. M.J. Taylor *et al.* to be published.
27. M.A. Bentley *et al.*, Phys. Rev. Lett. **97** 132501 (2006)
28. J.R. Brown *et al.* Phys. Rev. C **80** 011306 (2009) (Rap. Comm)
29. D.J.Morrissey *et al.* Nucl. Instrum. Meth. Phys. Res. B **204** 90 (2003)
30. D. Bazin *et al.* Nucl. Instrum. Meth. Phys. Res. B **204** 629 (2003)
31. J.A. Sheikh, P. Van Isacker, D.D. Warner and J.A. Cameron, Phys. Lett. B **252** 314 (1990)
32. E. Caurier *et al.*, Phys. Lett. B **75** 2466 (1995)
33. S.M. Lenzi *et al.*, Z. Phys. A **354** 117 (1996)
34. F. Brandolini *et al.*, Nucl. Phys. A **642** 387 (1998)
35. E. Caurier, Code ANTOINE, Strasbourg, 1989-2005; E. Caurier and F. Nowacki, Acta Phys. Pol. B **30** 705 (1999)
36. T. Otsuka, M. Honma, and T. Mizusaki, Phys. Rev. Lett. **81** 1588 (1998)
37. D.M. Rae, Nushell, http://knollhouse.eu
38. E. Caurier, G. Martínez-Pinedo, F. Nowacki, A.Poves, and A.P. Zuker, Rev. Mod. Phys. **77** 427 (2005)
39. T. Otsuka, M. Honma, T. Mizusaki and N. Shimitzu, Prog. Part. Nucl. Phys **47** 319 (2001)
40. W. Kutschera, B.A. Brown and K. Ogawa, Riv. Nuovo Cimento **31** 1 (1978)
41. A. Poves *et al.*, Nucl. Phys. A **694** 157 (2001)
42. M. Honma,T. Otsuka, B.A. Brown, and T. Mizusaki, Eur. Phys. J. A **25** 499 (2005)

43. B.H. Wildenthal, Prog. Part. Nucl. Phys **11** 5 (1984)
44. B.A. Brown, and B.H. Wildenthal, Ann. Rev. Nucl. Part. Sci. **38** 29 (1988)
45. B.A. Brown and W.A. Richter, Jour. Phys.: Conference Series 20 (2005) 145
46. E. Caurier, K. Langanke, G. Martínez-Pinedo, F. Nowacki, and P. Vogel, Phys. Lett. B **522** 240 (2001)
47. P. Mason *et al.*, Phys. Rev. C **71** 014316 (2005)
48. F. Della Vedova *et al.*, *AIP Conf. Proc.* 764, 205 (2005)
49. Y. Utsuno, T. Otsuka, T. Glasmacher, T. Mizusaki and M. Honma, Phys. Rev. C **70** 044307 (2004)
50. M. A. Bentley and S. M. Lenzi Prog. Part. Nucl. Phys **59** 497 (2007)
51. S.M. Lenzi *et al.*, Phys. Rev. Lett. **87** 122501 (2001)
52. A.P. Zuker, S.M. Lenzi, G. Martinez-Pinedo and A. Poves, Phys. Rev. Lett. **89** 142502 (2002)
53. J. Ekman *et al.*, Phys. Rev. Lett. **92** 132502 (2004)
54. J.A. Cameron *et al.*, Phys. Lett. B **235** 239 (1990)
55. D.D. Warner, M.A.Bentley and P. Van Isacker, Nature Phys. **2** 311 (2006)
56. M.A. Bentley *et al.*, Phys. Rev. C **62** 051303 (2000)
57. A. Poves, J. Phys. G **25** 589 (1999)
58. M.A. Bentley, *et al.*, Phys. Lett. B **437** 243 (1998)
59. D.R. Inglis, Phys. Rev. **82** 181 (1951)
60. L. Trache *et al.*, Phys. Rev. C **54** 2361 (1996)
61. B.A. Brown and R. Sherr, Nucl. Phys. A **322** 1979 (61)
62. J. Ekman *et al.*, Eur. Phys. J. A **9** 13 (2000)
63. A. Gadea *et al.*, Phys. Rev. Lett. **97** 152501 (2006)
64. D.Rudolph *et al.* Phys. Rev. C **78** 021301 (2008) (Rap. Comm)
65. S.J. Williams *et al.*, Phys. Rev. C **68** 011301 (2003)
66. D. Tonev *et al.*, Phys. Rev. C **65** 034314 (2002)
67. R. du Rietz *et al.* Phys. Rev. Lett. **93** 222501 (2004)
68. F. Della Vedova *et al.*, Phys. Rev. C **75** 034317 (2007)
69. D.G. Jenkins *et al.*, Phys. Rev. C **72** 031303 (2005)
70. F. Della Vedova *et al.*, Legnaro National Laboratory Ann. Rep. 2003, INFN (REP) 202/2004 p.3
71. M.A. Bentley *et al.*, Phys. Rev. C **73** 024304 (2006)
72. R. Orlandi *et al.*, Phys. Rev. Lett. **103** 052501 (2009)
73. R.G. Thomas. Phys. Rev. **88** 1109 (1952)
74. J.B. Ehrman. Phys. Rev. **81** 412 (1951)